Michigan State University

National Superconducting Cyclotron Laboratory

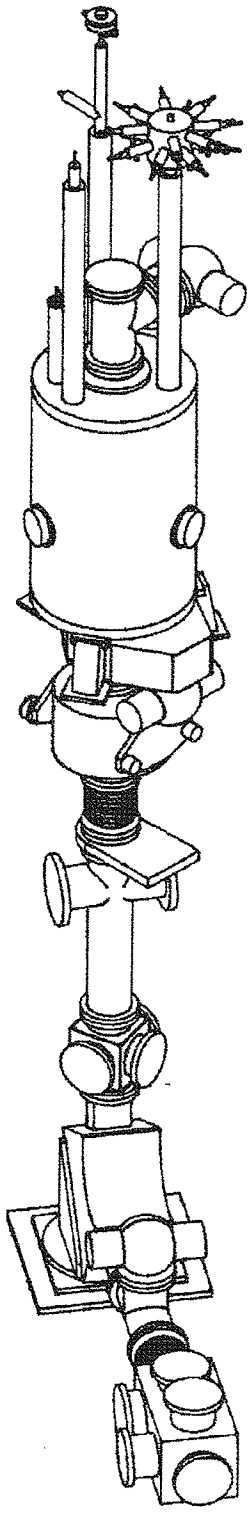

K500 Cyclotron High Intensity Injection for the Coupled Cyclotron Project

T.A. Antaya

NSCL

MSUCP- 76

K500 Cyclotron High Intensity Injection - for the Coupled Cyclotron Project

T.A. Antaya

15 April 94

1. Introduction

This report is concerned with the ion production and the low energy beam transport (LEBT) requirements of the K500 cyclotron for this coupled cyclotron proposal. In this paper, we will present the requirements in each of these areas and present our plans for meeting them. At the present time, the electron cyclotron resonance ion source (ECRIS) still represents the state-of-the-art for the production of continuous beams of intense multiply-charged ions, and best approaches the ion production requirements of this proposal. Yet, these requirements will stimulate significant further development of the ion source and LEBT capabilities at NSCL. The development of a radically new High B operating mode on our SCECR ion source [1] permits us to explore this regime, and considerable experimental progress has already been made as will be presented. The existing LEBT systems for cyclotron injection at NSCL as elsewhere were designed before it was known that space charge could play an important role in the transport of intense beams extracted from ECRIS [2]. In order to meet the K500 injection requirements of this proposal, a new space charge compensated injection line will be built.

The NSCL cyclotrons are now injected by an ECRIS/LEBT facility, as shown in Figure 1.1. This facility consists of three ECRIS with complimentary capabilities, a coupling switch-yard that permits any (or all) ECRIS to be coupled to either cyclotron, and low energy beam transport lines to both the K500 and K1200 cyclotrons. With this facility, we have the ability to provide nearly all of over 100 developed beams in virtually any order, permitting complex beam scheduling that can respond rapidly to user's changing requirements. In 1993, on average, we changed beams about every 40 hours, and used up to three ECRIS to provide multiple beams in succession to single experiments. Since there are more sources than cyclotrons, this configuration permits ion source and beam development simultaneously with source operations. In the period 1991-1993, we introduced a new developed beam about every two weeks.

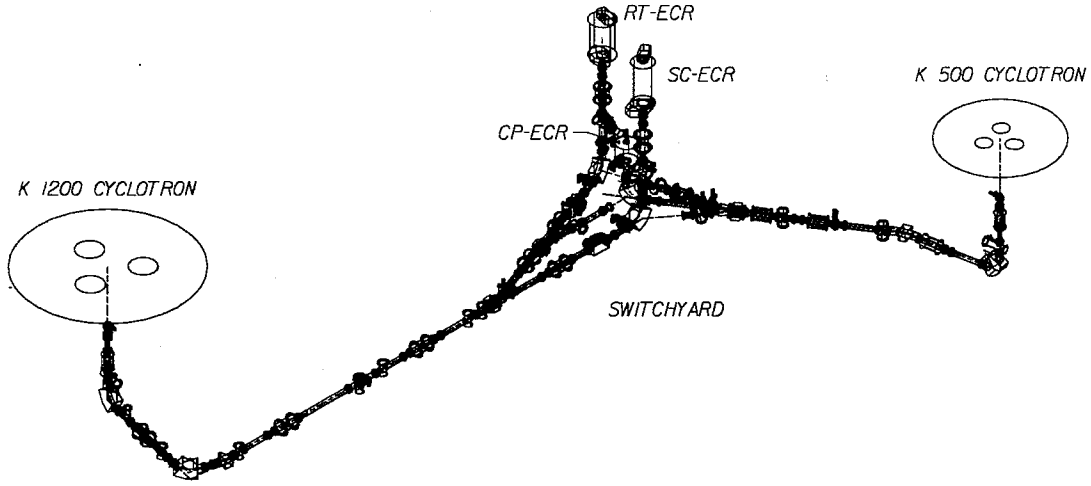

Figure 1.1: The existing low energy beam production and cyclotron injection facility at NSCL.

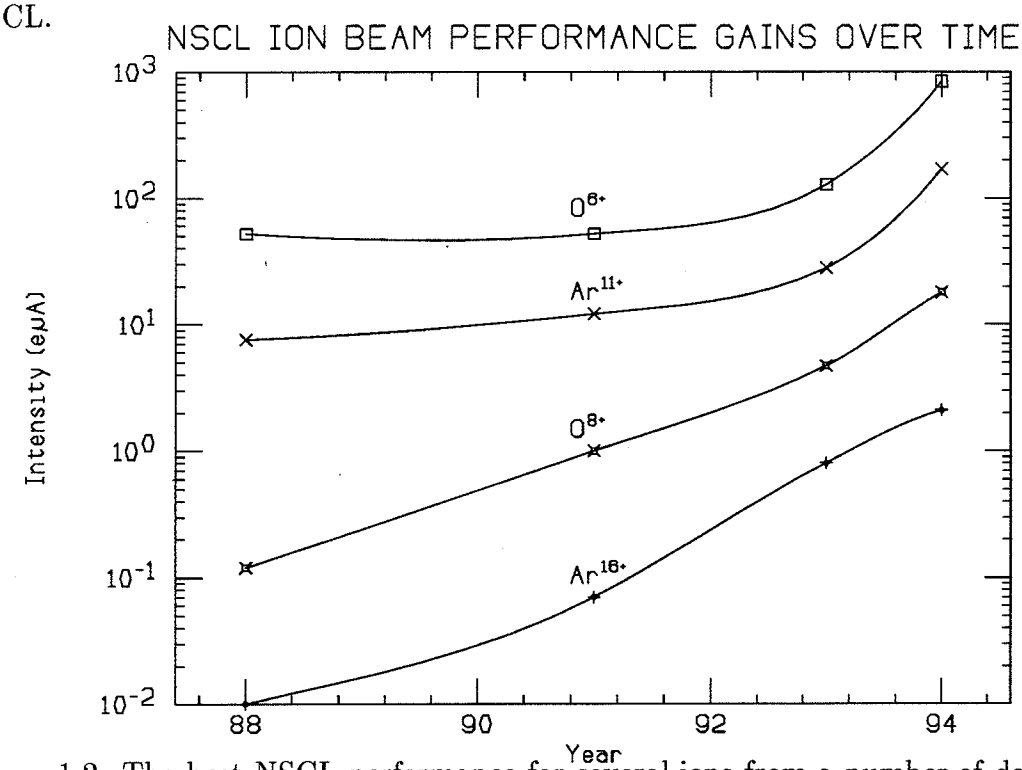

Figure 1.2: The best NSCL performance for several ions from a number of developments is tracked for several years.

The three ECRIS shown in Figure 1.1 have a broad range of capabilities. The RTECR, designed for high performance and low material consumption, can produce intermediate and highly charged ions of all species. The CPECR, with a metal vapor stage and a heated main stage liner, is designed for alkali metal beams, particularly lithium, but can also produce exotic molecular ions like HeH+ and HeD+, important for the production of low energy hydrogen and deuterium beams in the K1200 cyclotron. The SCECR, with a full superconducting coil set, has the widest dynamic tuning range, and the highest performance of these sources, when operating in the High B mode.

The historical, the primary developmental emphasis here has been the production of increasingly higher energy cyclotron beams, which for all species, generally means extending the useful level of ion source intensity to successively higher charged ions. We hold the world record for the highest charge ion (U 39+) injected without stripping from an ion source into an accelerator [3]. More recently, with the development of the A1200 fragment separator, a new emphasis has been placed on the development of intense intermediate energy beams for secondary beam production. Such beams are transmission-intensity limited, rather than ion production limited, and we started an effort to study and develop intense low velocity beams for cyclotron injection [4]. Additionally, there has been a major effort to develop beams of rare stable elements to enhance the production of particular neutron or proton rich secondary beams. This has led to the development of an ECRIS metallic ion beam technique, Super Gas Mixing, of considerable importance to the successful production of such beams [5]. We have as a consequence the ability to produce ions of all species, from hydrogen to uranium, including rare isotopes with fully stripped ions available to $Z \simeq 18$, and high Z ions with charge states up to 40+. Figure 1.2 shows the performance gain with time for several selected ions over a number of source developments. Intensities have increased 1-2 orders of magnitude in this time period, with higher gains occurring for more highly charged ions. In all cases, the intensities labelled 1994 represent world records for ECRIS.

With three operating sources, the ECRIS effort at NSCL is at present one of the largest world-wide, a consequence of the operating requirements of the experimental program on the K1200 cyclotron and its demands for continually enhanced performance. At the same time, all NSCL ECRIS designs have been directly copied at other nuclear science laboratories [6][7][8][9].

2. Ion Production Requirement for the Coupled Cyclotron Proposal

The ion production requirements for K500 cyclotron injection will be discussed first.

Ion	A	K500 Inject Q1	ECRIS Required Performance (pμA)	SCECR Present Performance (pμA)	RTECR Present Performance (pμA)
O	16	3	50	180	30
S	36	6	30	30†	6
Ar	40	7	30	30	6
Ca	48	8	50	50†	10
Kr	84	15	8.0	8.0	1.5
Kr	84	14	8.0	8.0	2.0
Xe	129	22	3.6	3.6	0.3
Xe	129	21	3.2	3.2	0.35
Au	197	29	0.9	0.9†	0.10
Au	197	26	1.8	1.8†	0.20
U	238	32	0.5	0.5†	0.04
U	238	28	1.0	1.0†	0.1

Table 2.1: The coupled cyclotron proposal required ion source performance versus present SCECR performance († indicates estimated performance).

2.1. Ion Source Requirements

Representative ion source requirements for the coupled cyclotron project are given in Table 2.1, along with the present performance of the SCECR and RTECR ion sources. The intensities necessary to meet the specified performance goals have been chosen to be equal or less than those already achieved at the NSCL. For light ions like oxygen, the final intensity from the K1200 cyclotron is 1 particle microampere (pμA), and the available performance exceeds that of the proposal. For heavier ions, the present SCECR performance is assumed. For comparison, the present performance of the RTECR, now the basis for the K1200 beam program, is also given in Table 2.1.

In ECRIS, the plasma is initiated through the ionization of a gas at low pressure. To make ions of metallic species in an ECRIS, one generally starts with a 'support gas' plasma, and introduces by some auxiliary technique the metal in solid or vapor form. Since metals are generally more reactive than gases (otherwise they would be gases), the group chemistries of the periodic table can play a role in the ultimate performance for metallic species. The selected metallic ion production intensities in Table 2.1 assume that there is no penalty for metallic feed materials over gaseous feed materials. As we will show in Section 2.2.2, we have already developed a metallic ion technique that provides the same performance as for gaseous feed.

Table 2.1 also includes ^{48}Ca, a species with low natural abundance. It is assumed that this species is available 100% enriched, and that it can be used in an enriched form without

a performance penalty. Since such highly enriched forms can be prohibitively expensive, an additional requirement is placed on the ECRIS metallic ion production technique that it have high material use efficiency for such beams. One of the main loss modes for metallic ions in an ECRIS is condensation on the inner wall of the plasma chamber. This condensation can alter the source performance. Low material consumption would also insure that there is less possibility for source poisoning.

In this proposal, we also preserve the option to operate the K1200 cyclotron stand-alone. In that mode of operation, the general requirements of: all species, continuous beams, rare isotopes, etc., are still the same as those desired for the coupled cyclotron mode. Since the final maximum energy and/or intensity will be substantially higher in the coupled mode, the facility limits will not be reached in the K1200 stand-alone mode. Therefore, stand-alone mode will have no additional impact on overall ion source requirements.

The ECRIS emittance should also match the K500 cyclotron acceptance, in order for these assumed intensities to be fully utilized, but we defer the discussion of starting ion beam requirements to Section 3.

2.2. ECRIS High Intensity Ion Production

Electron cyclotron resonance ion sources originated in thermonuclear fusion studies in the 1970's [10], but have been developed largely for application in nuclear physics laboratories. The initial drive for this development was the production of highly charged ions to obtain higher final energy beams from cyclotrons than were possible then with conventional ion source technology, while exploiting the other desirable features of the ECRIS: no cathodes, higher stability and reproducibility [18]. Since most ECRIS development has centered on the optimization of the highest obtainable charges of each species, little is known about the optimization of intermediate charge ions. One can observe however, that intermediate charge ions not near atomic shell limits can be more difficult to optimize, since ions are produced by successive electron impact ionization in ECRIS and the relative difference in ionization difficulty among electrons in the same sub-shell is small [12]. Of course, even less is known about intense intermediate charge metallic ion production in ECRIS than gaseous ion production.

For typical gaseous feed species, Figures 2.1 and 2.2 compare the highest performance ECRIS (NSCL SCECR [1], 18 GHz Minimafios [13], the 10GHz Caprice 2B at Grenoble [14], Riken [15], LBL AECR [16] and Jülich ICIS [17]) for the production of oxygen and neon ions. As can be seen, for most of these sources the intermediate charge ion performance is unreported. The two highest performance sources are the SCECR and the Grenoble 18 GHz Minimafios, with the SCECR having a slight edge. While optimized for highly charged ions, both of these sources have higher intensity performance for intermediate *and* highly charged ions, and though not shown, these trends hold for all heavier mass species as well. We can then say that high intensity intermediate charge performance is related to high charge state performance in ECRIS. Thus, the long term efforts to optimize ECRIS to make highly

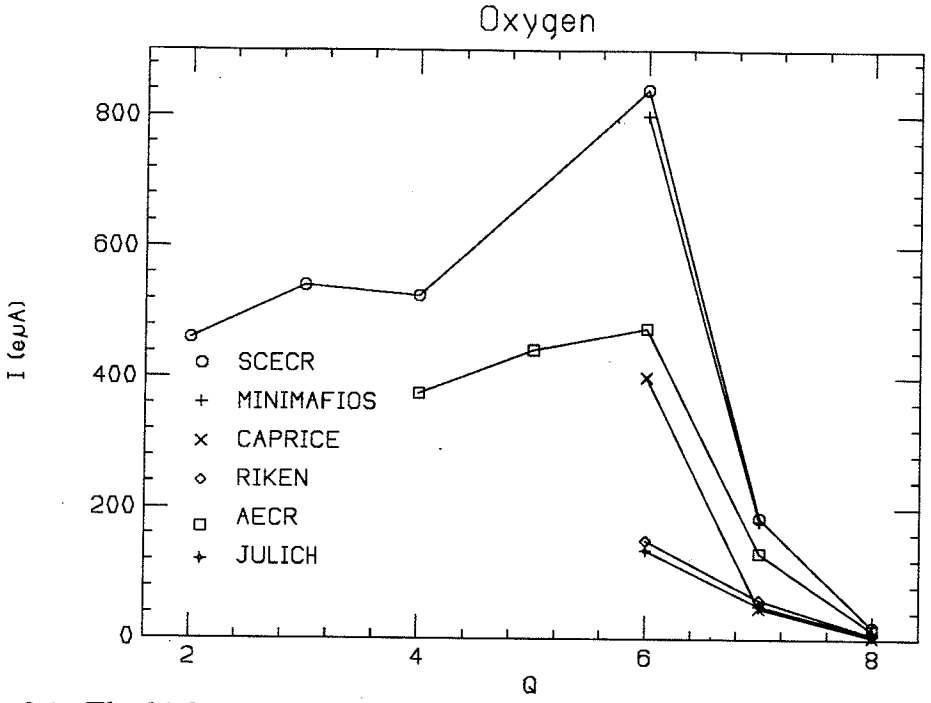

Figure 2.1: The highest performance ECRIS are compared for oxygen ion production.

charged ions has also resulted in sources that can produce intense intermediate charge ions, more important for the coupled cyclotron proposal.

When compared to other kinds of ion sources, it is generally agreed that ECRIS are more stable and reproducible, and that this is the consequence of using a large volume, electrodeless discharge to produce multiply-charged ions. This stability and reproducibility are essential for injecting cyclotrons. In this regard, larger ECRIS are generally more stable and uncritical than smaller ECRIS, as anyone who had ever tuned the largest operating source, ECREVIS at Louvain-la-Neuve, would know [11]. All of the ECRIS in Figs. 2.1 and 2.2 are compact ECRIS with the exception of the SCECR and ICIS, having confined plasma volumes about an order of magnitude larger than the other sources in this high performance group.

The 18 GHz Minimafios ECRIS was the result of a series of developments in Grenoble directed at demonstrating the existence of a frequency scaling rule for ion production. In this theory, the plasma density $n_e \propto \omega_{ecr}^2$, where ω_{ecr} is the frequency of the microwaves injected into the plasma, and ion production rate R_q should scale with plasma density and ion confinement time as $R_q \propto n_e \tau_q$. In fact, the Grenoble group was able to demonstrate an increased total extracted intensity and higher maximum charge states in a series of ECRIS with increasing operating frequency from 10 GHz to 18 GHz, culminating in the above mentioned 18 GHz Minimafios [19]. To go beyond 18 GHz would require the use of superconducting magnetic technology in the ion source, not within the technical capabilities of the Grenoble group. There was some question that this frequency scaling theory was being

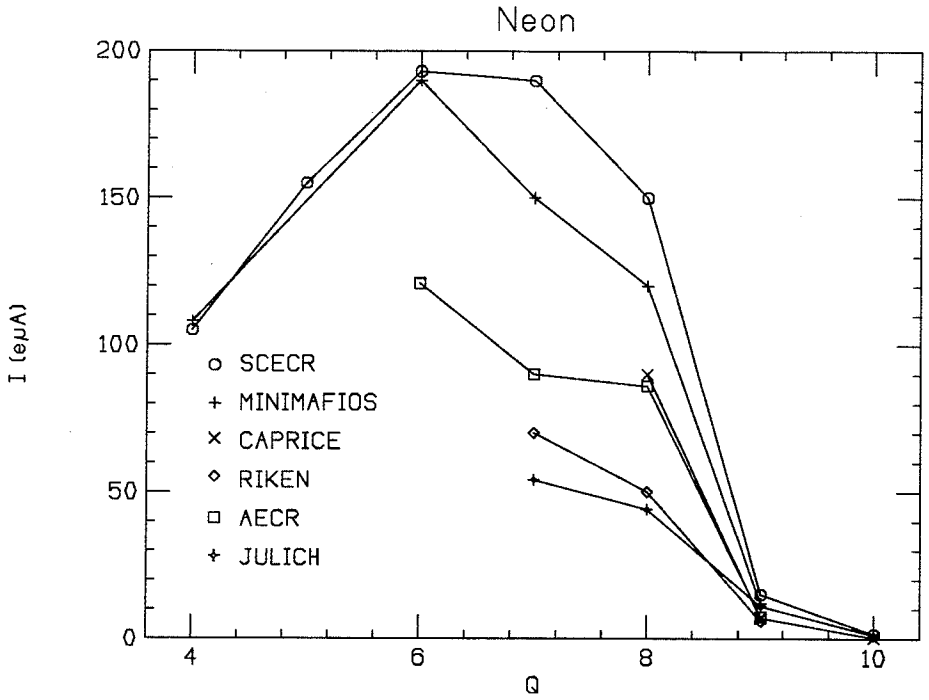

Figure 2.2: The highest performance ECRIS are compared for neon ion production.

incorrectly applied in ECRIS – the assumptions in this theory included that the plasma be non-collisional and non-magnetized, both invalid assumptions for an ECRIS plasma. Hence, there was a need to independently corroborate the Grenoble results, and if correct, take the next step to the higher frequency regime. It was for these reasons that the SCECR project was conceived at NSCL [20]. By using a fully superconducting coil set to generate the confinement field in the SCECR, it would be possible in one ECRIS to go from low to high frequencies to compare ion production performance. At the same time, the SCECR would be capable of operating in new regimes of magnetic confinement at lower resonance frequencies. The SCECR does indeed have performance equal to or exceeding the 18 GHz Minimafios, but at an operating frequency of only 6.4 GHz when the magnet is adjusted to have very high mirror confinement [21]. This new High B mode of the SCECR has shown that the performance scaling in ECRIS is an ion confinement scaling, not a frequency scaling of the plasma density [1]. The sharp upward trend in NSCL ion production versus time in 1993, as shown in Figure 1.2, is a direct consequence of the SCECR High B mode, and we feel it is the most promising ECRIS operating mode to exploit in meeting the ion production requirements of this coupled cyclotron proposal.

2.2.1. Baseline Gaseous Feed Performance– SCECR High B Mode

The SCECR is shown in schematic form in Figure 2.3. The overall source design follows the design of the RTECR at NSCL. Figures 2.4 and 2.5 show the design and optimized operating

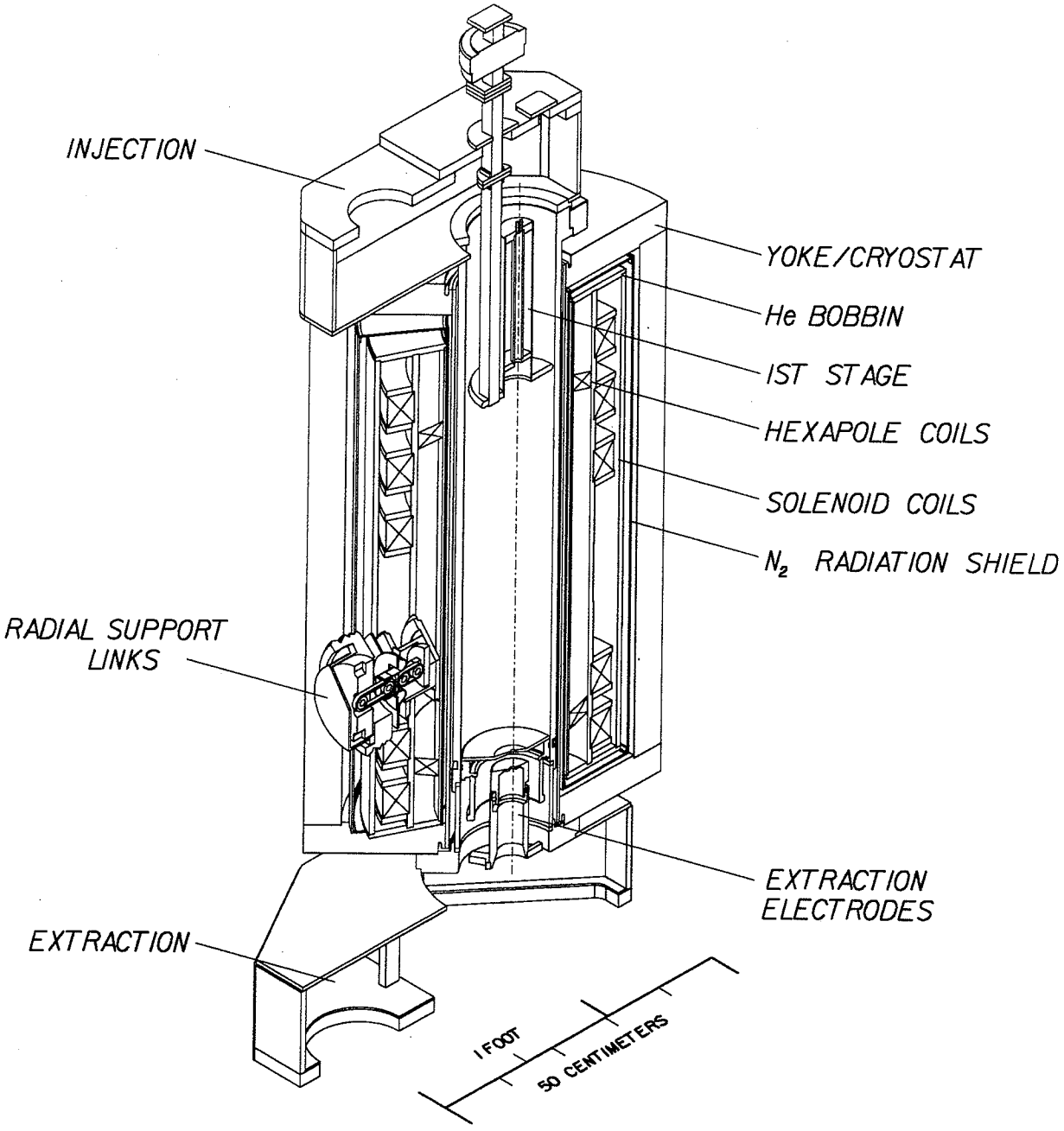

Figure 2.3: The SCECR has a full superconducting magnet, permitting variable frequency operation. At low resonance frequency, there is then a wide dynamic range in magnetic confinement. From this feature the High B mode was developed at 6.4 GHz.

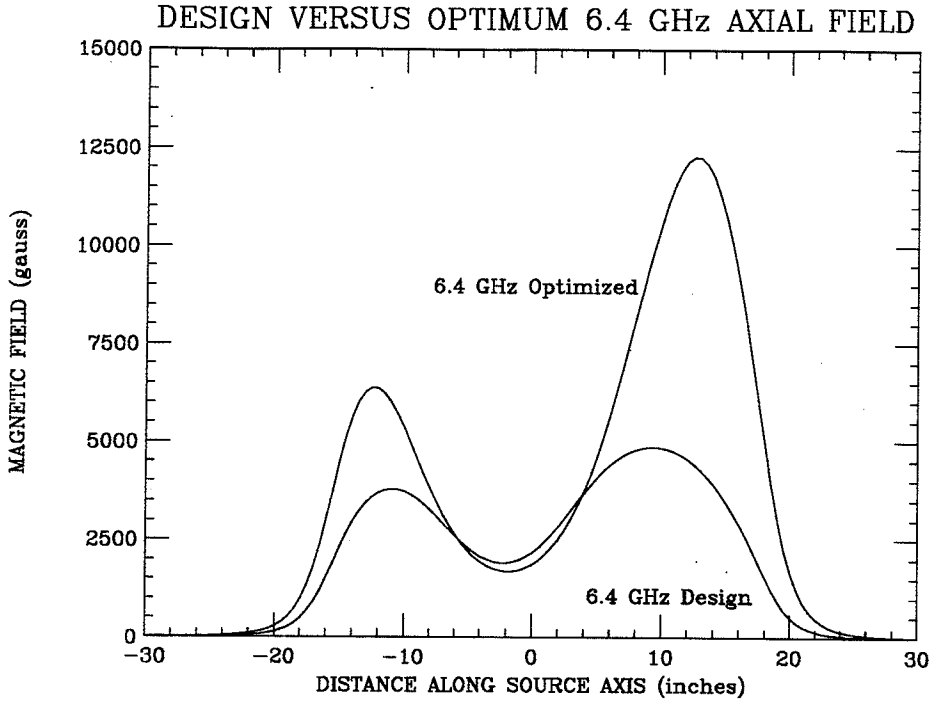

Figure 2.4: The designed and optimized 6.4 GHz axial magnetic fields of the SCECR are shown.

axial and radial magnetic fields for 6.4 GHz operation. The design fields are identical to the RTECR, and are also close to the norm for quasi-single stage operating modes in ECRIS. When operated at 6.4 GHz, the SCECR high charge state performance always optimizes at much higher axial and radial confinement fields, also shown in these two fields plots. The maximum optimized fields are in fact closer to the operating fields of the higher frequency sources ($\sim$ 14 GHz), and that, coupled with the much larger plasma volume of the SCECR and lack of criticality, allows much higher performance than is possible in these sources. In order to see the impact of operating with significantly higher magnetic confinement than is the norm in ECRIS, Figure 2.6 compares the krypton performance of the RTECR and SCECR, when both are operated at 6.4 GHz. For a given charge, there is an order of magnitude or more increase in intensity. At fixed intensity, the observed krypton charge state shifts upward by 6-8 charges.

Other qualitative operating characteristics are improved when operating the SCECR in the High B mode over conventional ECRIS operating modes. The well-known ECRIS plasma stability improves further with the higher confinement, and this is directly seen in the stability of extracted beams. Ion beam currents extracted for the SCECR can be constant to two or three decimal places. With higher magnetic confinement, both the plasma density and the average electron energy in the plasma are higher, so the ion production rate is higher than in other ECRIS – both the peak intensities and maximum observed charge states are enhanced, as was shown, for example, for krypton in Figure 2.6. The ionization efficiency

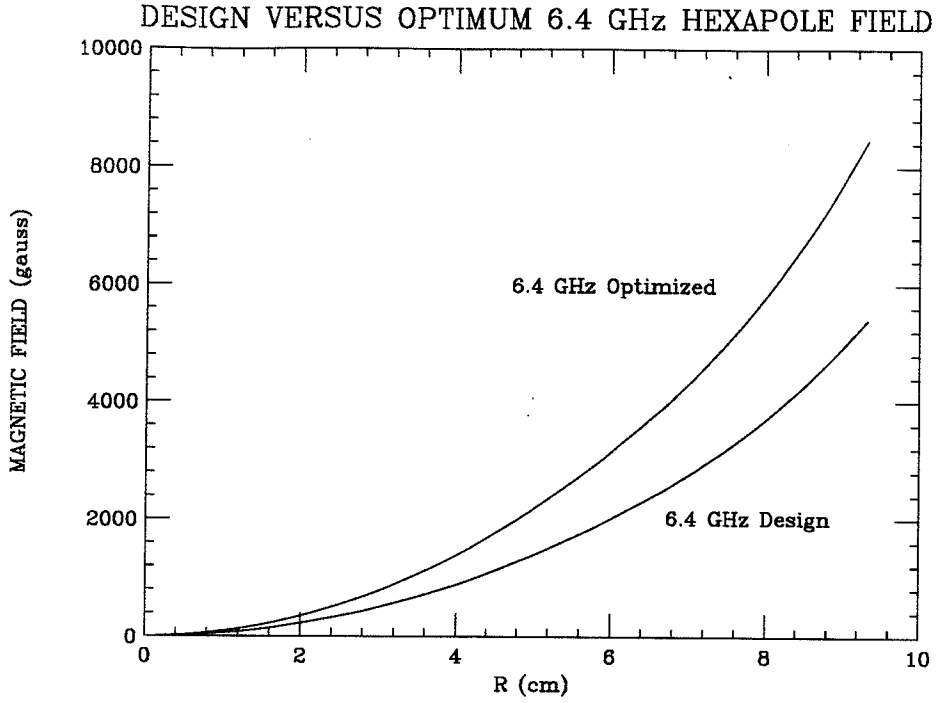

Figure 2.5: The design and optimized 6.4 GHz radial magnetic fields of the SCECR are shown.

in the SCECR is high and also partially a consequence of operating in the High B mode. With the Altas Ion Source Group, we have measured absolute ionization efficiencies in the SCECR of 70-80% [22], a desired feature critical to efficient utilization of enriched isotope feed materials.

While the ion source requirements of the coupled cyclotron operating mode presently match the capabilities of the SCECR operating in the High B mode, we do not believe that work on the High B mode is done– in fact it is just beginning. We will continue to push the development of this mode to higher levels of performance, particularly for heavy species, where the final beam intensity is strongly limited by the available source performance. The present operating field is near the limit for effective first harmonic electron cyclotron resonance heating at 6.4 GHz. In order to go to even higher levels of magnetic confinement, the operating frequency must be raised! So the next step will be to develop a High B mode of operation at 14.5 GHz. The required 14.5 GHz microwave is already available at NSCL, but the magnet will require some additional work. This development will follow the initial development of a metallic ion capability in the SCECR.

2.2.2. Metallic Ions - The Super Gas Mixing Technique

For metallic ion production for the coupled cyclotron proposal, we require:

- a technique(s) to cover all metallic species

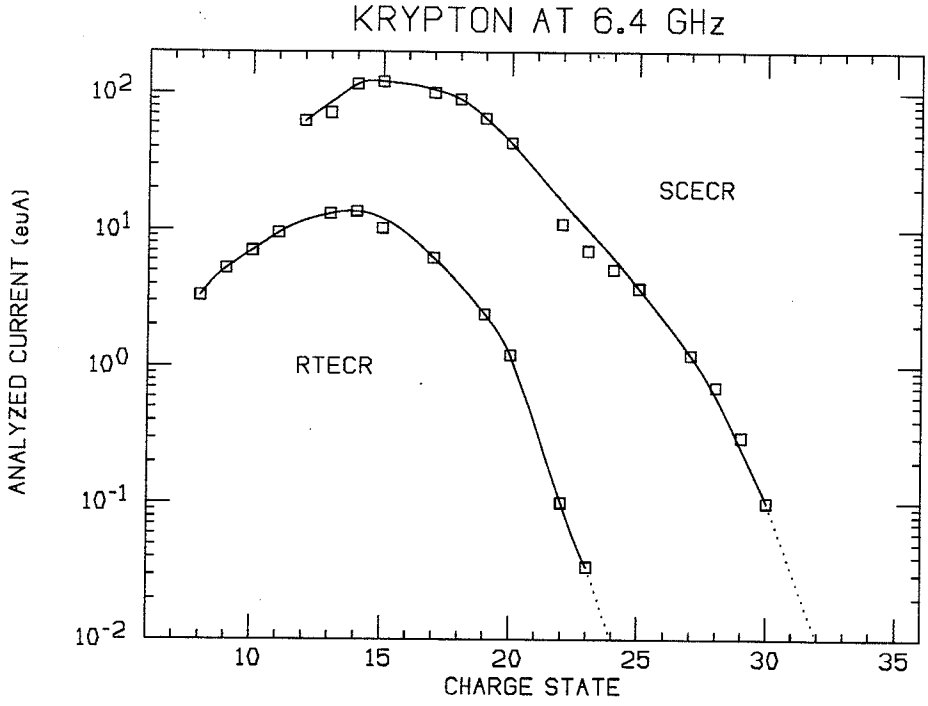

Figure 2.6: The impact that the High B mode has on source performance can be seen in this comparison of the SCECR and the RTECR for krypton ion production. The RTECR was the starting point for the design of the SCECR – at low field they are structurally equivalent.

RTECR Metal Ion	**Consumption Material**	**K1200 Energy (MeV/u)**	**Consumption Rate (mg/hr)**
$^{48}Ca^{16+}$	CaO powder	100	<.07
$^{58}Ni^{15+}$	metal powder	70	-
$^{92}Mo^{25+}$	metal powder	70	-
$^{106}Cd^{26+}$	CdO powder	60	.058
$^{197}Au^{35+}$	metal film	35	-
$^{238}U^{39+}$	UO powder	25	<.14

Table 2.2: Highly charged metallic ions for K1200 accelerated beams, produced via Super Gas Mixing in the RTECR.

- performance equivalent to gaseous feed species
- very high ionization efficiency to permit utilization of enriched rare isotopes
- ionization of enriched isotopes in their available form where feasible to minimize conversion losses.
- avoid ion source poisoning

We have already developed a metallic ion technique with such properties in the RTECR, the Super Gas Mixing Technique [5], and need only apply it to the SCECR High B mode of operation. The RTECR is shown schematically in Figure 2.7. It has radial main stage ports that permit the direct insertion of solid materials into the plasma, as shown in Figure 2.8, and this serves as the basis for the Super Gas Mixing technique. This technique originated as an attempt to use this system to make an intense $^{92}Mo^{25+}$ beam for an isotope search experiment at the K1200 cyclotron [23]. The natural abundance of ^{92}Mo is 15%. To obtain sufficient beam intensity, our starting point therefore was 100% enriched metal powder. We tried various techniques to turn this powder into a metal flake for direct plasma insertion, but had trouble with material consumption (too high), or the charge state distribution (too low). At the same time, this metal powder is too refractory to place in an oven for vaporization. We did find that powder would stick to the end of a small diameter (4 mm) alumina rod. This alumina rod could be directly inserted into an oxygen plasma in the RTECR main stage, with very good success, if the oxygen plasma had been set up in the following manner:

- The RTECR is pre-tuned on $Xe+O_2$ to maximize the xenon high charge states (27-31+).
- The xenon gas feed is shut off.
- The oxygen feed rate is increased above that in the optimized $Xe+O_2$ mixture to raise the mainstage pressure 1/2 order of magnitude.
- The microwave power is doubled, but the source magnetic field is held constant.
- An alumina rod is coated with approximately 10 mg of ^{92}Mo, then inserted radially into the RTECR main stage plasma, just until some low charge molybdenum ions are observed in the source output.

With this technique, one ends up with a relatively uncritical high pressure, low charge state oxygen plasma, having a superimposed high peaked metallic ion charge state distribution as an impurity. This represents the extreme limit of the well known gas mixing technique in ECRIS [24]. Table 2.2 shows a number of highly charged metallic ion beams produced via this technique in the RTECR and accelerated in the K1200 cyclotron. As

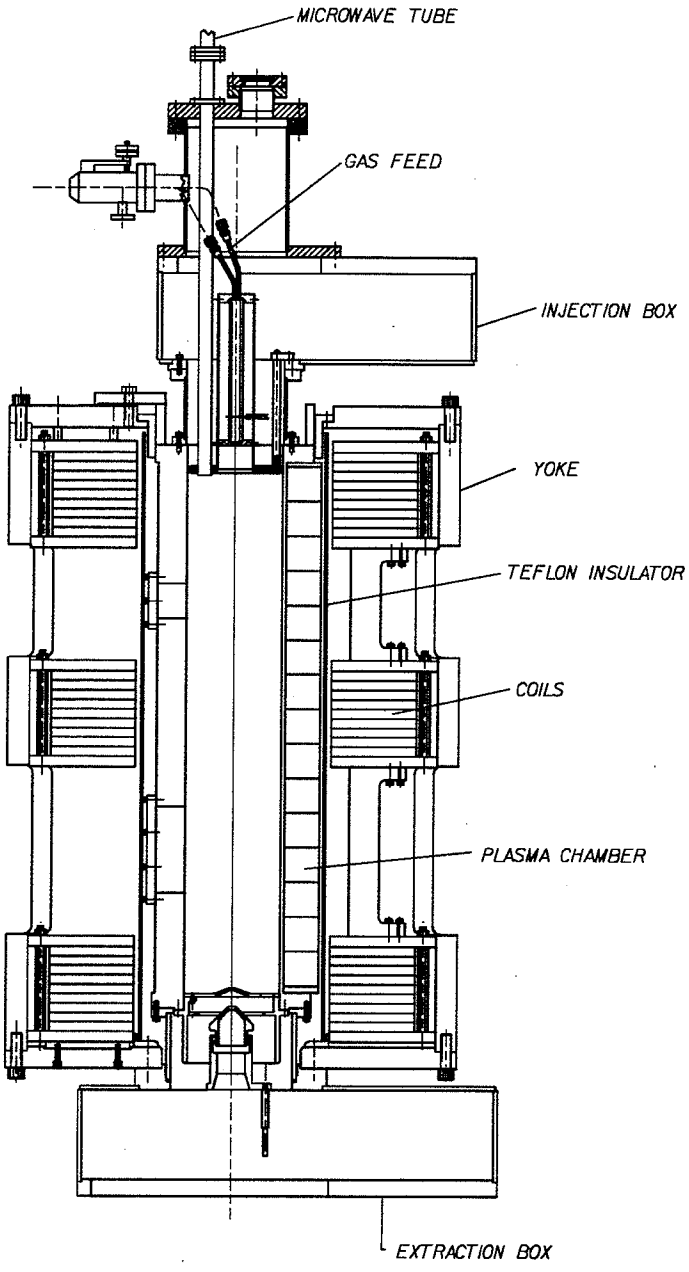

Figure 2.7: The RTECR source shown here, is used for the production of heavy metallic ions at NSCL.

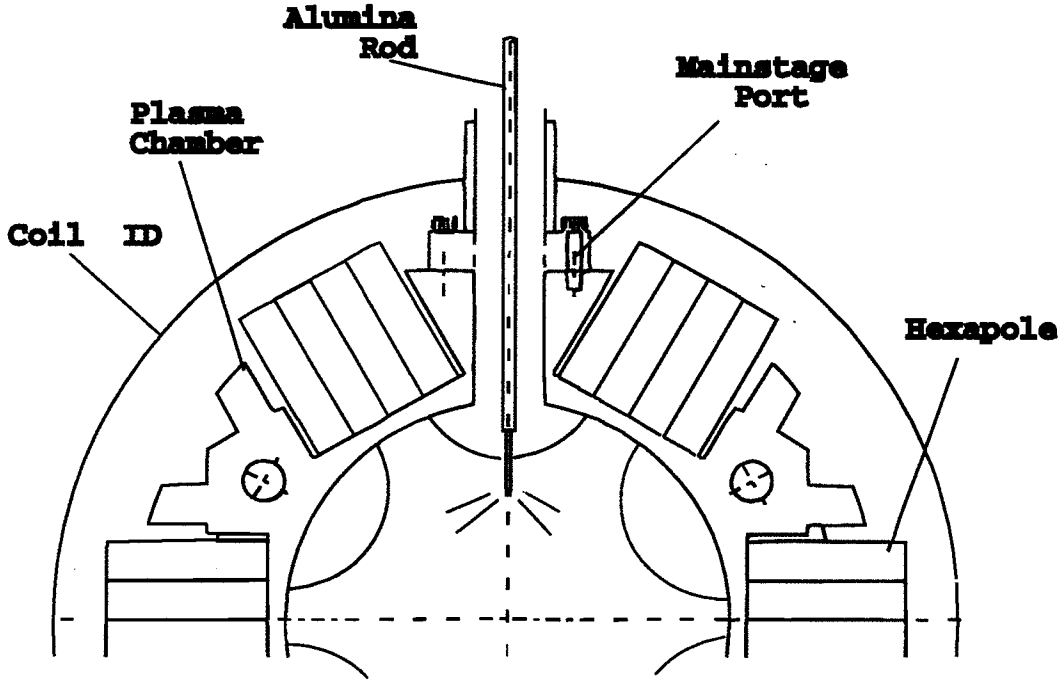

Figure 2.8: In the super gas mixing technique, a small amount ($\leq$ 10 mg!) of metallic species is introduced directly into the main stage oxygen plasma on the end of a movable ceramic rod.

can be seen in Table 2.2, the technique is independent of the available enriched form. In addition, the material consumption is quite low, with a 10 mg charge lasting 100 hours or more. With little material introduced into the plasma chamber, contamination is unlikely, and source poisoning is not an issue. With a consumption rate of the order of 1 μgm/min in most cases very rare isotopes can be utilized without exorbitant cost. The use of an alumina feed rod and an oxygen plasma are important in this technique. The alumina rod does not electrically perturb the oxygen plasma, and also apparently thermally isolates the metallic sample. We do not see a breakdown of the alumina under bombardment by energetic electrons in the plasma, though the metallic material on the tip is effectively vaporized. The oxygen plasma evidently keeps the metallic vapor from recondensing on the plasma chamber walls by a reactive gas process, eliminating a major loss mechanism for metallic vapor under normal circumstances in an ECRIS. Finally, as Figure 2.9 shows, the overall source performance achieved is also completely independent of the origin of the feed material– the RTECR performance scaling is smooth in Z from neon to uranium, dependent on the physics of successive electron impact ionization, and not the chemistry of the feed materials.

2.2.3. SCECR Modification for Metallic Ions

At present, the SCECR has only produced ions of gaseous species. For the metallic ion species of this coupled cyclotron proposal, we plan to extend the RTECR Super Gas Mixing Technique to the SCECR. Since the SCECR does not have radial ports, the access to the main stage plasma for sample heating will be from the top, as shown schematically in Figure 2.10. The present solid feed system on the RTECR allows only one sample in the ion source plasma chamber. The SCECR solid feed design shown in Figure 2.10 has provision for six samples. This affords some redundancy for a single species metallic beam run, or for beam production from a sequence of several different metallic species in one run. It is anticipated that the metallic ion production performance of the SCECR will increase over that of the RTECR in the same manner as it did for gaseous species, such as was shown previously for krypton ion production in Figure 2.6.

2.2.4. Multiple Sources Are Required

In the present K1200 stand-alone operating mode, typically one source provides a beam to the cyclotron while another source is being set up for a second beam or is being developed for a new beam. Additionally, since the capabilities of the existing sources partially overlap, there is a level of redundancy built into the system should one source not be operational for any reason. This simultaneous operation and development has been an important feature of present facility operation. We expect this need to continue, but given that we believe the SCECR High B mode best matches the coupled cyclotron requirements, all sources in the coupled mode should have ultra-high intensity intermediate charge ion capabilities.

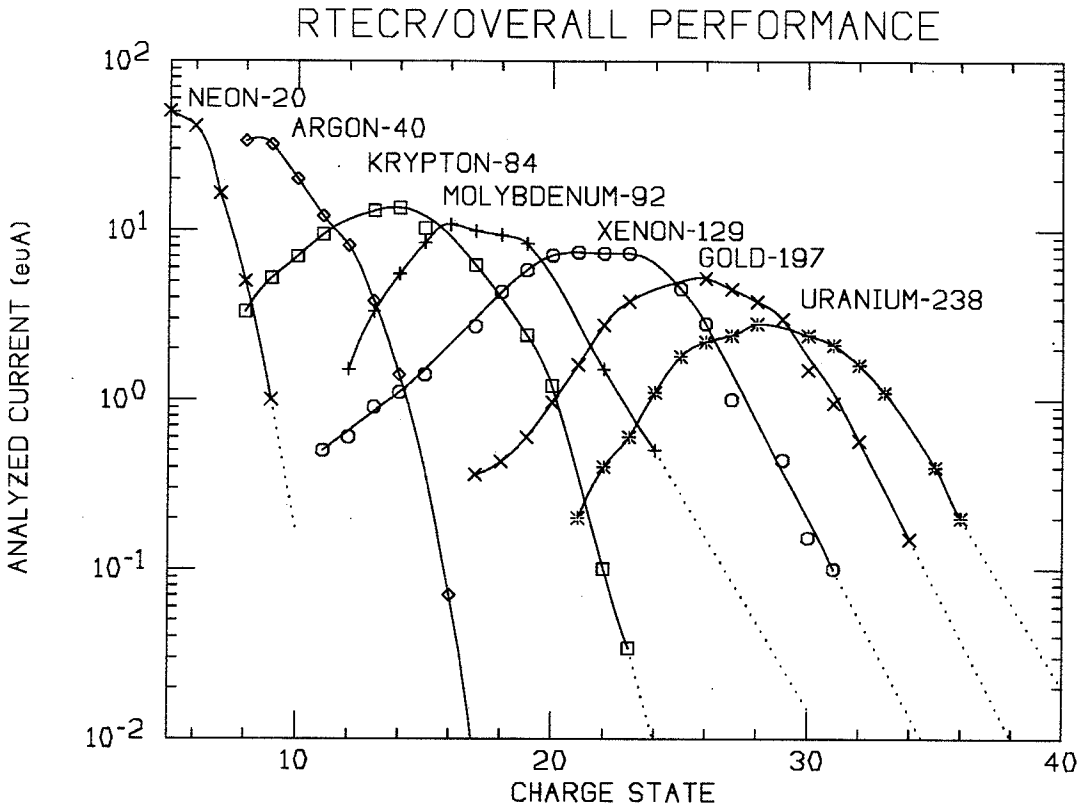

Figure 2.9: The overall performance of the RTECR for gaseous and metallic species is shown. As can be seen, the performance is smooth in Z, and is independent of the material feed origin.

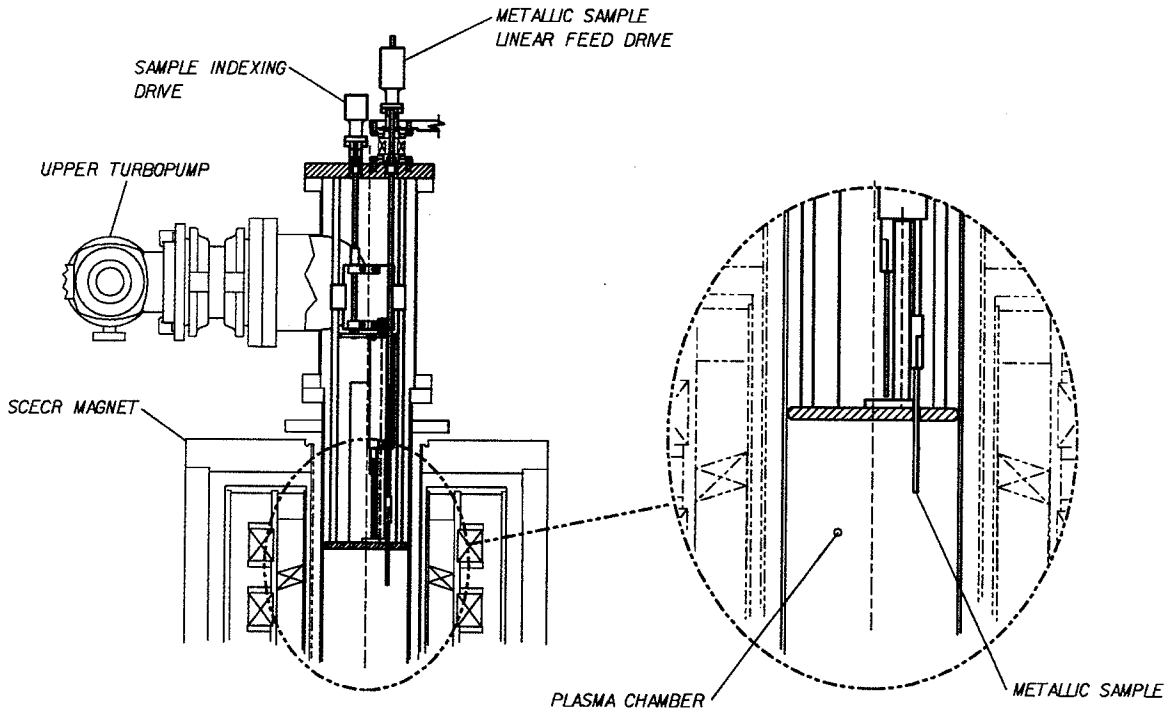

Figure 2.10: To make metallic ions via the super gas mixing technique in the SCECR, the upper pumping structure must be removed and an axial sample drive system is installed.

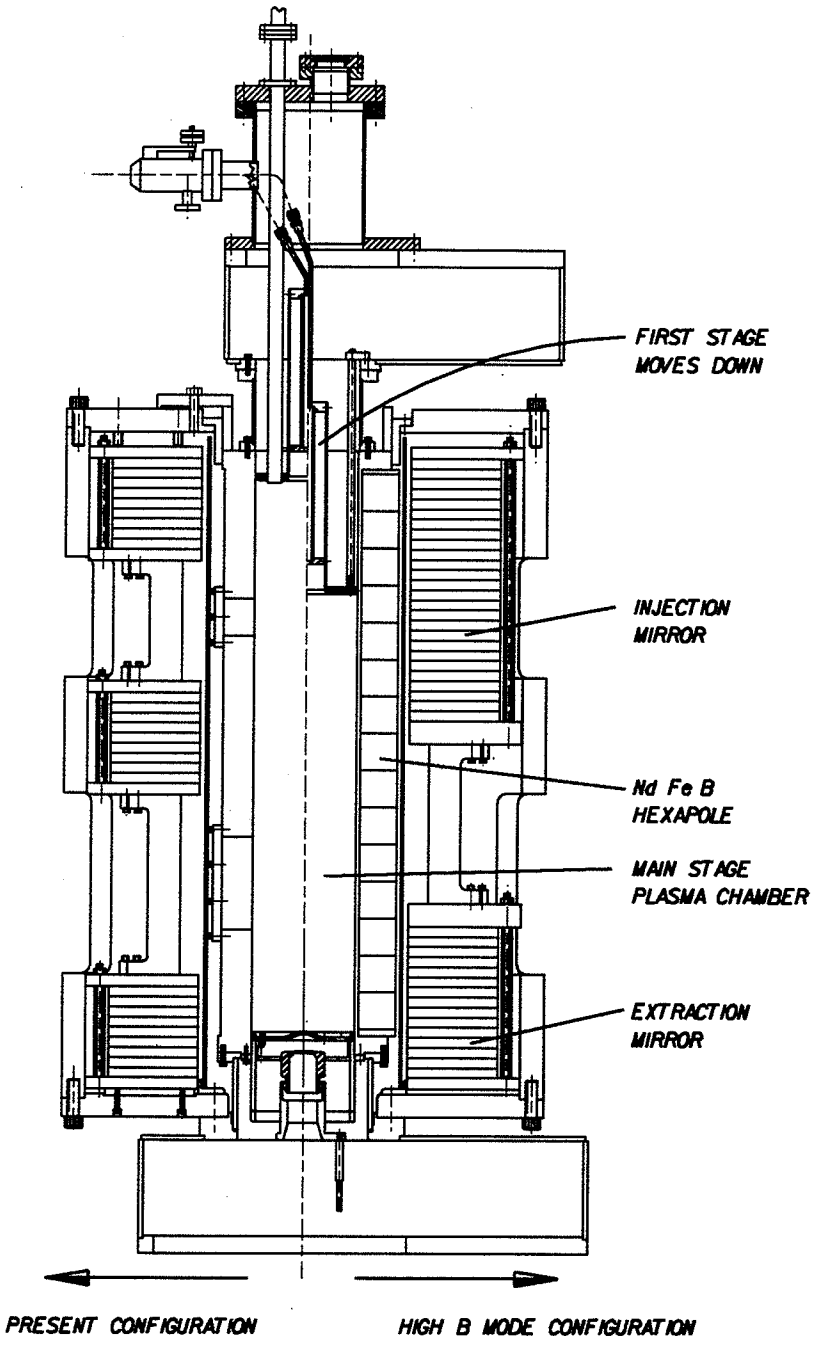

Figure 2.11: In this diagram the present configuration of the RTECR is shown on the left, with the proposed High B mode configuration on the right.

2.2.5. RTECR Modification for High B mode Operation

While developed with a superconducting magnetic system on the SCECR, the 6.4 GHz High B mode field can be made with conventional magnet technologies. In fact, as Figure 2.11 shows, the NSCL RTECR can be modified in a straight forward way to operate in the High B mode at 6.4 GHz. The $SmCo_5$ hexapole magnet is replaced by a higher energy product NdFeB permanent magnet structure in order to obtain the required 0.5 T radial confinement field. The three present axial mirror coils are reconfigured into two axial mirrors with increased amp-turns to produce an approximation to the required axial confinement field. The gas/microwave injection stage is moved down to the location found to be optimum for the SCECR. This modification of the RTECR is expected to yield performance like the SCECR High B mode for a cost of approximately 1/4 of that required to build a second SCECR. This would then give us two high intensity ECRIS to apply to beam production for the coupled cyclotron operating mode.

2.2.6. The CPECR

The CPECR at NSCL is a low intensity source that does not match the requirements of the coupled mode operation, and it is not foreseen that it will be used in the coupled mode. It has an important alkali metal ion production capability that we would transfer to the RTECR.

2.3. Proposed ECRIS Configuration

In summary, our plan is to operate the SCECR and an upgraded RTECR for coupled mode ion injection into the K500. The SCECR would be further developed to have a metallic ion capability following the Super Gas Mixing technique. We would continue to develop the SCECR High B mode to higher levels of magnetic confinement where additional gains in peak intensity and maximum charge states are anticipated. The CPECR operation would be discontinued and the alkali ion beam capability would be transferred to the 6.4 GHz High B mode RTECR. We would preserve the option to inject the K1200 directly for stand-alone operation, probably from the SCECR. This concept is shown schematically in Figure 4.1. The SCECR is shown with an analysis magnet in a rotating table, as in the present ion source facility. To move the SCECR from the K500 to the K1200 requires decoupling the beam line after the dipole and rotating the magnet. Controls and interlocks switch automatically from one beam line to the other. The time required to make the change is the pumpdown time for the analysis beam line only– the SCECR and the main beam lines remain under vacuum during the move.

Other coupled mode facility constraints will also affect the ion source/injection facility. The additional high energy shielding requirements, and the cyclotron coupling line to the facility will push into space presently occupied by ion sources power supplies and controls.

These will have to be relocated, and while this move will be somewhat logistically complex – it involves all the power supplies and controls – it is not viewed as a major issue.

3. K500 Cyclotron High Intensity Injection

The K500 cyclotron ion injection requirements will be met by the development of a new space charge compensated LEBT design, as will be presented in this section. Space charge limited transmission is not generally considered an issue for multiply-charged positive ion beam transport, as the available intensity is generally much lower than for singly-charged ion beams. ECRIS break new ground for the production of intense continuous beams of multiply-charged ions, exceeding the performance of all other existing ion source types, with intensities now approaching milliampere levels for multiply-charged ions. Thus more ion beam current is available for accelerator injection than has been previously possible from positive ion sources. At the same time, ECRIS operate at low pressure (about $10^{-7} Torr$), and the beam line pressure must be equally low, else the beamline residual gas load would represent the main feed source for ion production. The beamline pressure must also be low to avoid recombination losses of multiply-charged ions transported away from the ion source. This low beamline pressure suppresses the source term for electron production in beam collisions with the residual gas, by as much as four orders of magnitude lower than for conventional (higher pressure) positive ion sources. As a consequence, we believe that these intense multiply-charged ions *do not* fully neutralize in the beamline, and for proper transport, this space charge must be accounted for in the LEBT design. For the coupled cyclotron proposal, the primary issue is to transport with minimal losses, the maximum brightness that can be accepted by the K500, while avoiding space charge induced aberrations that dilute the phase space.

3.1. Ion Injection Requirements for the Coupled Mode Operation

The coupled-mode operation beam requirements for K500 injection are:

- Q/M $\leq$ 0.2
- V $\leq$ 30 kV
- I $\leq$ 0.5 emA
- Dc Transmission (source analyzed to K500 spiral inflector) = 50%
- Transverse emittance $\epsilon_x, \epsilon_y \leq 75\ \pi$ mm·mrad

The LEBT design must satisfy several important functional requirements:

1. Take beams downward from the vertical ECRIS and bend them 90° into the horizontal plane
2. Transport beams through the tunnel and cyclotron vault to the K500 axis
3. Bend the beam vertically 90° to the matching point on the K500 axis for non-axis injection

The first section of the LEBT, serves as well as the mass analysis system for the ECRIS. For source tuning, low charge states to M/Q = 40 must be observable at a standard source tuning voltage, establishing the required analysis rigidity; and for species identification, a nominal resolving power of about 2 cm / % momentum is required. The horizontal beam transport section must preserve the starting emittance and permit beam magnification adjustments as required to match the cyclotron axial injection. The distance of the horizontal beam transport line below the cyclotron median plane is taken to be the present 3.5 m (lowering the LEBT would be difficult and costly, and raising it would expose the beam to a higher magnetic fringe field from the cyclotron.) The cyclotron end of the horizontal beam transport section must have provision to correct for beam deflection by the cyclotron fringe field. The match point for cyclotron injection is taken to be 3 m below the cyclotron median plane. This location is just above the last horizontal to vertical bend. Therefore any beam magnification adjustments required to match the axial injection starting emittance must be accomplished in the horizontal section. The LEBT must include beam defining slits, faraday cups and emittance/profile measure devices as necessary to optimize the injection process, sufficient steering elements to maintain the beam centering, and secure beam stops for personnel and equipment safety interlocks.

3.2. ECRIS Beam Characteristics

How large should the emittance from an ECRIS be? In ECRIS, ions are extracted from a three dimensional Minimum B magnetic structure [10], and we take this as a starting point for the development of a theoretical estimate for the expected emittance. In the RTECR, this Minimum B field is obtained through the superposition of a 30cm bore $SmCo_5$ hexapole with a warm bore tandem magnetic mirror [25], while in the SCECR, it is obtained from 15 cm bore superconducting hexapole and a 30 cm bore superconducting tandem mirror. In both of these sources the ion extraction aperture is a = 0.8cm. The solenoid field at the extraction aperture of both sources is azimuthally symmetric while the hexapole field has an azimuthal component with 3-fold symmetry. The hexapole field is near zero within the radius of the extraction aperture since $a/r_{hex} \ll 1$ and therefore does not play an important role in this initial beam formation process. Then also $\vec{A} = A_\phi(r,z)\hat{\phi}$ is valid within the extraction aperture, the hexapole not withstanding.

The Hamiltonian for this system is then:

$$H = \frac{1}{2M}(P_r^2 + \frac{P_\phi^2}{r^2} + P_z^2 + Q^2 A_\phi(r,z) - \frac{2Q}{r} A_\phi(r,z)) + QV \tag{3.1}$$

The total electrostatic potential (V) should have azimuthal symmetry, and include the extraction fields (ex) and the beam space charge (sp):

$$V(r,z) = V_{ex}(r,z) + V_{sp}(r,z) \tag{3.2}$$

The extraction electrode system is cylindrically symmetric, and assuming also that the space charge is as well, we note that

$$\frac{\partial H}{\partial \phi} = \phi \dot{P}_\phi = 0 \tag{3.3}$$

and hence that the azimuthal canonical momentum is a constant of motion. That is

$$P_\phi = p_\phi + QrA_\phi = \text{Const} \tag{3.4}$$

Further, one can show that the two transverse emittances are equal and given by

$$\epsilon_x = \epsilon_y = |P_{\phi_f}/p_{z_f}| \tag{3.5}$$

where $P_{\phi f}$ is the final azimuthal canonical momentum and p_{z_f} is the final z mechanical momentum. Furthermore, it is true that P_{ϕ_i} is maximum at $r = a$, so the maximum starting transverse emittance is

$$\epsilon_{max} = |P_\phi(r=a)/p_{z_f}| = a\left|\frac{Mv_\phi(a,o) + QA_\phi(a,o)}{p_{z_f}}\right| \tag{3.6}$$

In ECRIS positive ions have low thermal energies in the plasma, so if the extraction voltage is large ($K_Q \ll QV_{ex}$), then

$$p_{z_f} \simeq \sqrt{\frac{2QV_{ex}}{M}} \tag{3.7}$$

Introducing a thermodynamic temperature T_Q as

$$K_Q \equiv \frac{3}{2} T_Q \tag{3.8}$$

then

$$v_\phi = \sqrt{T_Q / M} \tag{3.9}$$

and we may rewrite the transverse emittance as

$$\epsilon = \epsilon_x = \epsilon_y = a[(\frac{T_Q}{2QV_{ex}})^{1/2} + A_\phi(a,o)\left(\frac{Q}{2MV_{ex}}\right)^{1/2}] \tag{3.10}$$

Eq. 3.10 shows that the emittance depends on both the starting thermal energy and the fact that the ions originate in a magnetic trap. There are two limiting cases:

$$\text{Hot Ions} \qquad \epsilon \approx a\left(\frac{T_\phi}{2QV_{ex}}\right)^{1/2} \tag{3.11}$$

$$\text{Cold Ions} \qquad \epsilon \simeq a^2 Q B_z(a,o)\left(\frac{Q}{2MV_{ex}}\right)^{1/2} \tag{3.12}$$

In Equation 3.12, we have assumed for the form of the vector potential that of an azimuthally symmetric magnetic field, given that for r < a, the hexapole field can be neglected.

In Table 3.1, we have a prediction of SCECR transverse emittances for oxygen and argon ion beams, based on the limits expressed in Eq. 3.11-3.12. In both cases, the emittance is seen to increase with increasing charge. Figures 3.1 and 3.2 show measured total emittances for oxygen and argon ion beams extracted from the SCECR. In both cases, for low charge ions, the absolute and normalized emittance is observed to increase with charge, as is predicted by our theoretical model. The measured emittances in Figs. 1.1 and 1.2 exceed the cold ion limit of Table 3.1 for low charge ions, and this is not a surprise. Ions in a multiply-charged ECRIS plasma are collisional and would be expected to have some initial thermal energy, and $5eV \cdot Q$ is about the right amount. For highly charged ions of both species, the absolute and normalized emittances decline with increasing charge, and this is not expected.

ION	COLD LIMIT mm.mrad	WITH T=5eV x Q mm.mrad
$^{16}O^{1+}$	77.	142.
$^{16}O^{5+}$	125.	190.
$^{16}O^{8+}$	152.	217.
$^{40}Ar^{1+}$	49.	114.
$^{40}Ar^{8+}$	96.	161.
$^{40}Ar^{14+}$	131.	196.

Table 3.1: The theoretical SCECR transverse emittance, calculated in the cold ion limit (Eq. 3.12), and including a nominal initial thermal energy, for some selected ions extracted at 0.4 T and 10 kV.

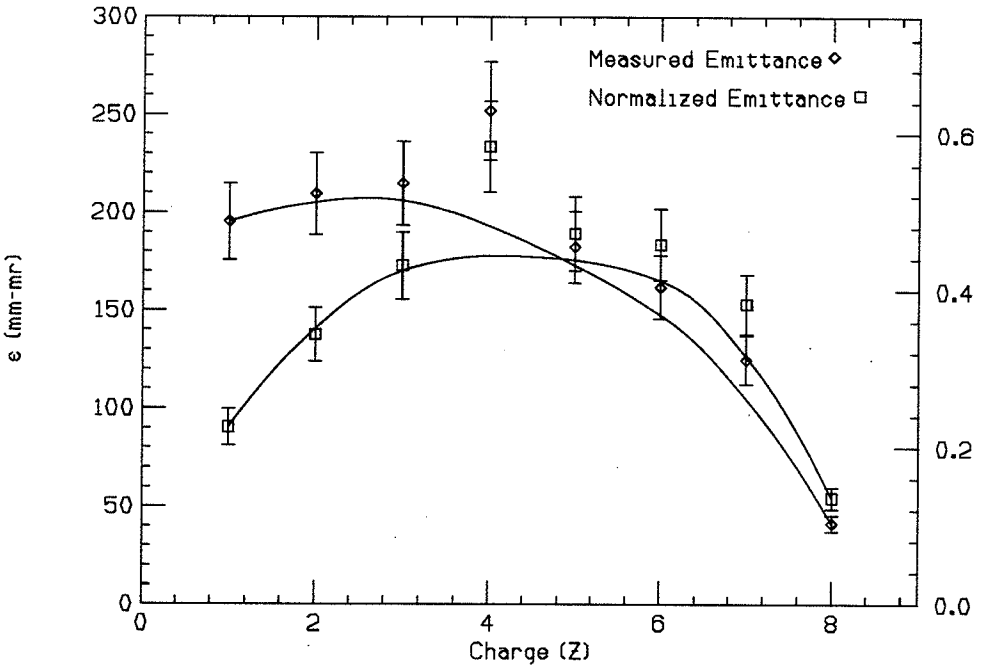

Figure 3.1: The measured and normalized emittances of oxygen ions extracted from the SCECR are shown. The intensity threshold is 100 % and the extraction voltage is 10 kV.

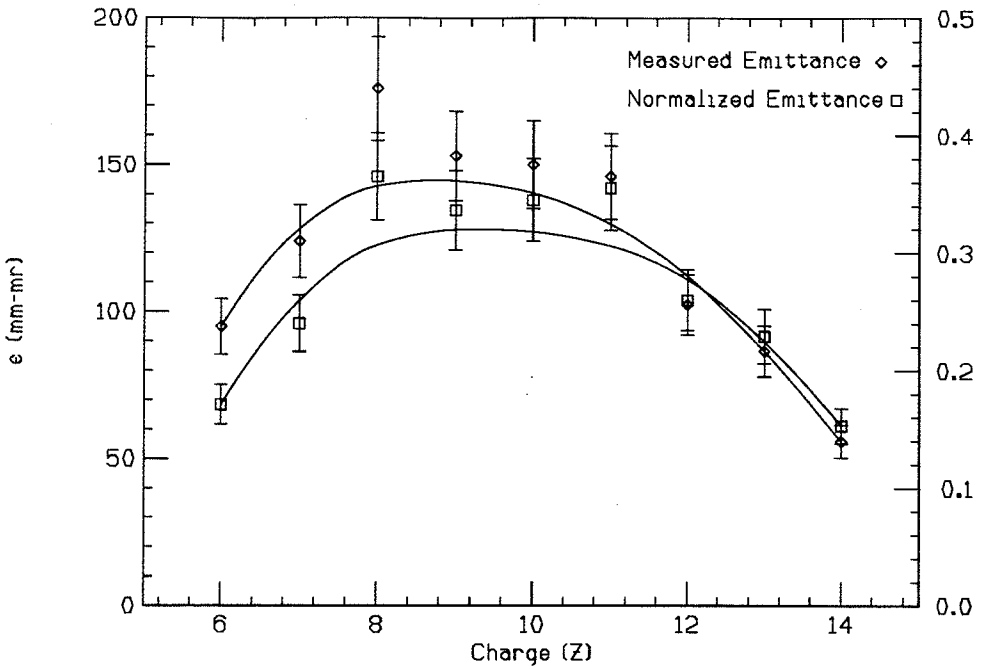

Figure 3.2: The measured and normalized emittance of argon ions extracted from the SCECR are shown. The intensity threshold is 100 % and the extraction voltage is 10 kV.

The a^2 dependence of the starting emittance is suspected – highly charged ions may have a much smaller starting radius than the extraction aperture, due to electrostatic confinement in plasma. In any case, for coupled-mode operation, the ions of interest are intermediate charge ions and these are seen as having the largest emittance.

The emittances shown in Figures 3.1 and 3.2 were obtained at a source bias voltage of $V_{ex} = 10kV$. According to Equation 3.10, the emittance should decline with $\sqrt{V_{ex}}$. Figure 3.3 shows the measure voltage dependence of O^{1+} ions extracted from the SCECR. At higher voltages, the $\sqrt{V_{ex}}$ dependence is seen. (At very low voltage beam, space charge blow-up of the beam in the analysis system results in a measured emittance substantially higher than the predicted.) Using this scaling for higher voltages, we can predict the emittance of ions like O^{3+} at a coupled mode K500 injection voltage of 30 kV, as shown in Figure 3.4. (The SCECR cannot presently operate above 18 kV, but we expect to be able to measure emittances at such voltages in mid-1994.) The measured absolute emittance of 225π mm·mrad at 10 kV would be expected to decrease to about 130π mm·mrad at 30 kV. If the source extracted emittance remains constant, the brightness of such ion beams will increase by at least a factor of 3 at coupled-mode injection voltages. (We anticipate an increase in brightness higher than that because an increase in the extracted ion current should occur as well.)

The measured SCECR emittances for selected cases are given in Table 3.2 for an extraction voltage of $V_{ex} = 10kV$, and scaled by $\sqrt{V_{ex}}$ for the 30 kV case. For example, the measured O^{3+} absolute emittance of 215π mm·mrad at 10 kV (see Figure 3.4) would be re-

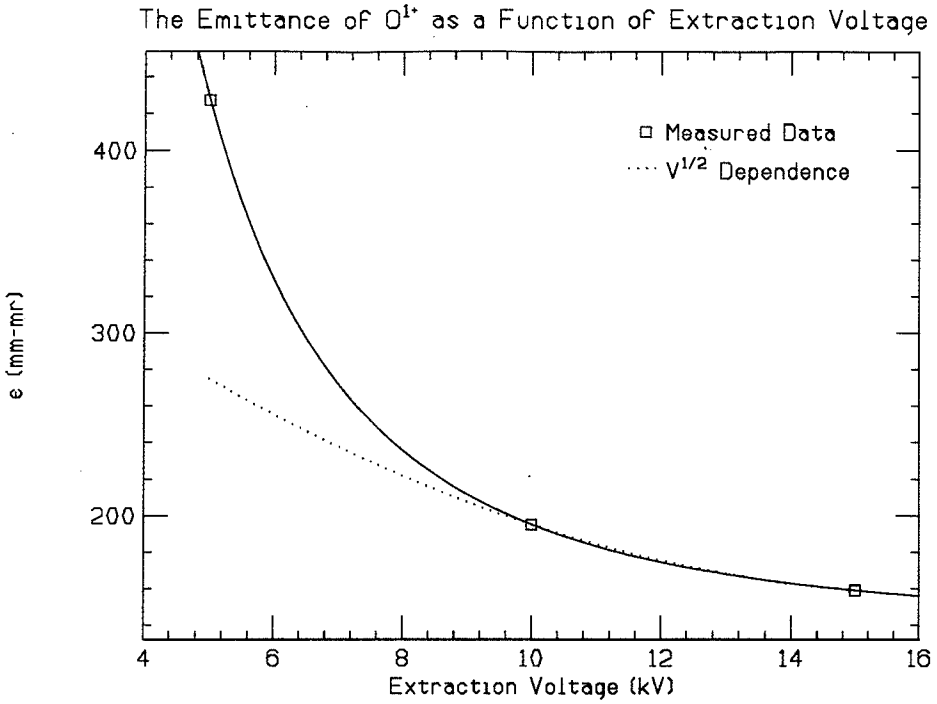

Figure 3.3: For high extraction voltages, the emittance of oxygen ions extracted from the SCECR follow the expected inverse velocity dependence, as shown here for O^{1+}. The deviation at low velocity for O^{1+} is due to aberations.

duced to 125π mm·mrad at 30 kV. Figure 3.5 shows the measured dependence of the SCECR O^{3+} emittance on intensity at 10 kV where $\sim$ 80% of the intensity is within an emittance of $130\pi\cdot$ mm·mrad. Hence at 30 kV, $\sim$ 80% of the intensity would be within an emittance of $75\pi\cdot$ mm·mrad. If this emittance can be transported to the cyclotron axis without aberrations, we would easily exceed the required 50% overall transmission criterion. The ion beams will be collimated to an emittance of $75\pi\cdot$ mm·mrad at a point just beyond the mass analysis system. No other significant losses are anticipated since the LEBT design admittance is large compared to the $75\pi\cdot$ mm·mrad. It is then anticipated that the ECRIS beam emittance at an operating voltage of 30 kV will provide beams of appropriate brightness for K500 injection in the coupled cyclotron system.

3.3. Space Charge Limited Beam Transport

Electron Cyclotron Resonance Ion Sources are now in use at about 40 laboratories world-wide for highly charged ion injection into accelerators for physics research [26]. Using this type of ion source, heavy ions with charge as high as 39+ have been injected directly into cyclotrons at intensities of a few hundred nanoamperes [27], as well as nearly fully-stripped light ions at intensities of a few hundred microamperes for cyclotron or synchrotron injection [28]. When compared to H- and H+ beam transport systems, these are not ion beam intensities

Ion	Measured at 10 kV π mm mrad	Scaled to 30 kV π mm mrad
$^{16}O^{1+}$	195	113
$^{16}O^{3+}$	215	125
$^{16}O^{5+}$	170	98
$^{16}O^{8+}$	40	23
$^{40}Ar^{1+}$	125	72
$^{40}Ar^{8+}$	150	87
$^{40}Ar^{14+}$	60	35

Table 3.2: The SCECR transverse emittance ($\approx 95\%$) measured at 10 kV and scaled ($1/V_{ex}^{1/2}$) to 30 kV for several ions.

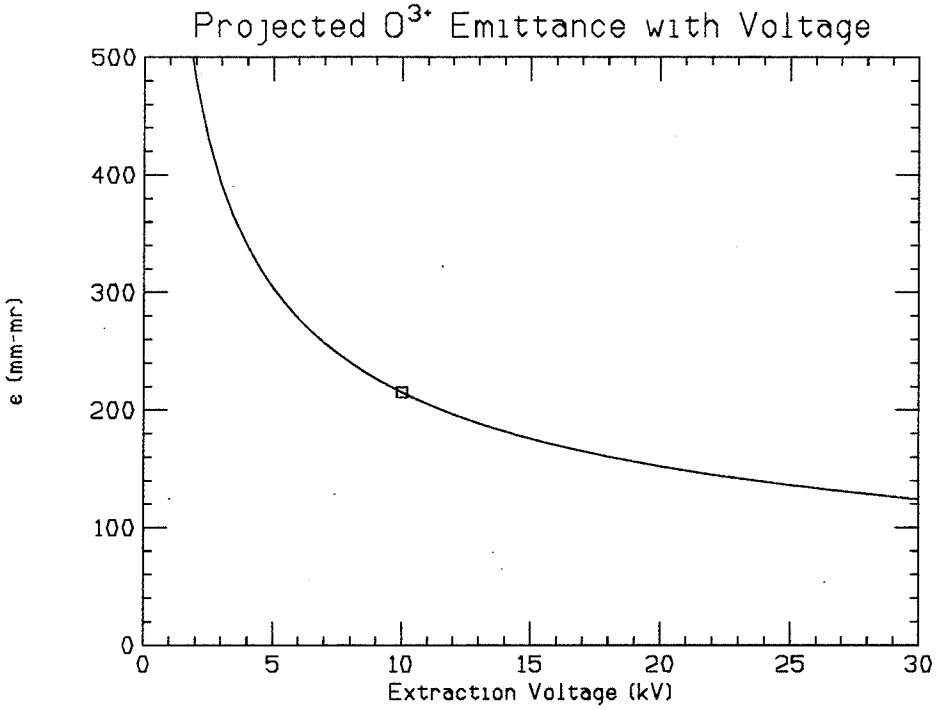

Figure 3.4: The expected scaling of the SCECR O^{3+} emittance with extraction voltage, normalized to the measured emittance at 10 kV.

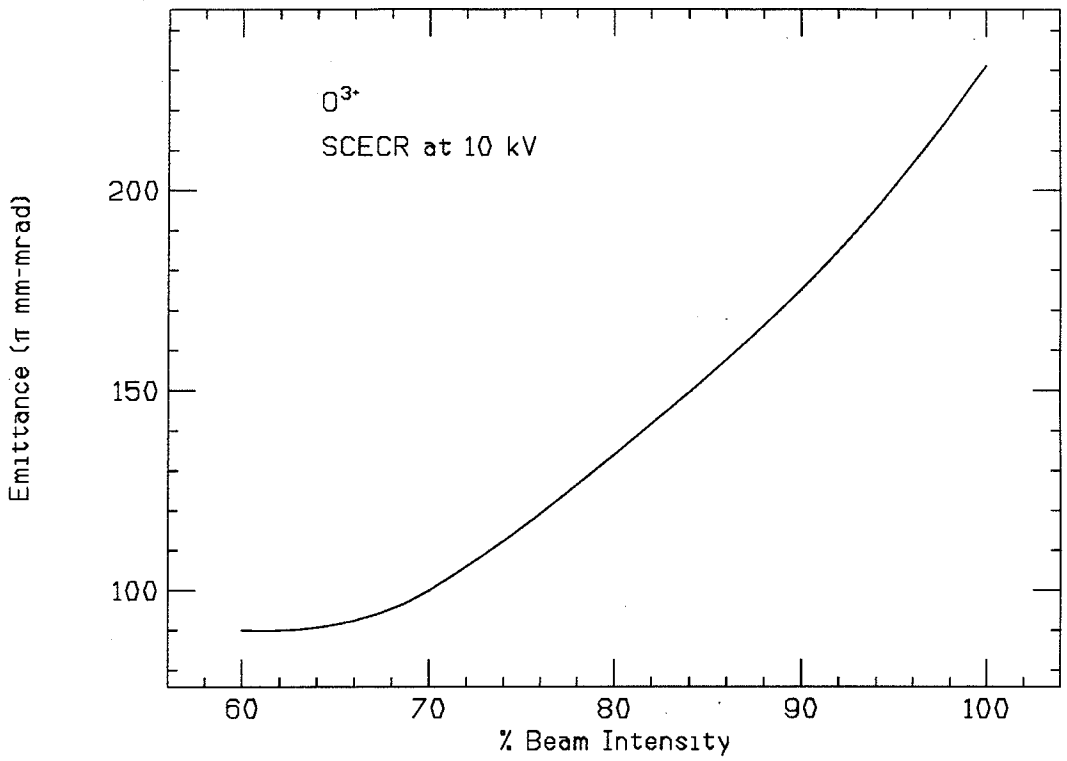

Figure 3.5: The dependence of O^{3+} emittance on intensity, extracted from the SCECR at 10 kV.

normally considered to be space charge dominated, and so a careful measurement of the initial beam properties should be sufficient to specify the beam transport system design and accelerator matching conditions. However, experimentally it is observed that both extremes – highly charged ions at low intensities and low charge ions at high intensities, exhibit sharp non-linear emittance growth in beam transport systems. This is true even in beam transport systems presumably having substantially higher designed acceptance than the initial beam emittance. In extreme cases, the overall beam transmission has actually been observed to decrease sharply with increasing beam intensity [29]. This mis-match has either been ignored or interpreted to imply that the initial beam characteristics were not well known. A more correct interpretation of this emittance growth is that it is a direct consequence of a non-linear growth in the beam envelope due to space charge forces. For proper matching of ECR ion source beams to accelerators, an aberration-free maximum beam intensity must be built

into the beam transport system.

3.3.1. Transmission Intensity Dependence – Existing Injection Lines

Highly charged positive ions produced by ECRIS are generally transported to the cyclotrons at energies of 5-20 $kV \times Q$, where Q is number of electrons removed. Without making too great a generalization, these LEBT share many design assumptions:

1. These beams are dc with particle currents of 0.001-30.0 pμA.

2. These beams are essentially monochromatic, thus $K_Q \ll QV_{ECR}$ where K_Q is the thermal energy of an ion of charge Q.

3. The transverse un-normalized emittances have been assumed to be symmetric, and of magnitude $\epsilon_x = \epsilon_y \leq 200mm \cdot mrad$ $\quad (\epsilon \equiv A_x/\pi!)$

While generally held to be valid, these assumptions have not been sufficient to properly design and transport ECR beams to accelerators.

3.3.2. Origin of the Space Charge Effect

While the coupled cyclotron performance depends on an SCECR class source, most of the fundamental ECRIS beam formation work done at NSCL has been done on the RTECR. The most complete set of argon emittance measurements performed on the RTECR are shown in Fig 3.12. The 90% emittance increases with charge but is about twice that expected on the basis of the cold ion limit of Eq. 3.12. The full emittance is much larger– half the emittance is contained in the last 10% of the current. The measured thermal energy of ions extracted from the RTECR is about $6eV \times Q$, and not sufficient to explain these large measured emittances. The acceptance of the beam transport system is $200mm \cdot mrad$ in both transverse planes [30], but the measured emittances exceed this acceptance. Therefore, aberrations may be causing an emittance growth —but what is driving the aberrations?

Beam simulations with BEAM3D [2] do explain the measured emittances if we assume that there is zero neutralization of the extracted beam, as we will now attempt to demonstrate. It is useful first to review how this is possible. If we view the dc beam as an ensemble of ions, then the total radial space charge force is a summation over all particles.

$$E_r = \frac{1}{2\pi\epsilon_o r}\sum\left(\frac{I_i}{v_{zi}}\right) \tag{3.13}$$

The equation of motion for an ion on the edge of a drifting azimuthally symmetric beam is then

$$P_r = \frac{P_\phi^2}{Mr^3} + \frac{Q}{2\pi\epsilon_o r}\sum\left(\frac{I_i}{v_{zi}}\right) \tag{3.14}$$

Integration once yields

$$v_r = \left[\frac{P_\phi}{M^2}\left(\frac{1}{r_m^2} - \frac{1}{r^2}\right) + \frac{Q}{\pi M\epsilon_o}\ln(\frac{r}{r_m})\sum(\frac{I_i}{v_{zi}})\right]^{1/2} \tag{3.15}$$

Where r_m is the initial beam radius ($r = r_m$) at $t = 0$. Observing that $v_\phi = P_\phi/M_r$ and defining $v_\perp \equiv \sqrt{v_\phi^2 + v_r^2}$, then we can write the transverse divergence of the beam as

$$\alpha_\perp = \left[\frac{P_\phi^2}{M^2 v_z^2 r_M^2} + \frac{Q}{\pi M\epsilon_o v z^2}\ln\left(\frac{r}{r_m}\right)\sum\left(\frac{I_i}{v_{zi}}\right)\right]^{1/2} \tag{3.16}$$

Equation 3.16 shows clearly that the beam surface will have a constant maximum transverse divergence if the space charge force is zero, that is, if $\sum(I_i/v_{zi}) \equiv 0$. This is of course the normal assumption in the LEBT design for ECR sources. One measures (or assumes) an initial maximum divergence at a waist after the ion source, and lets the beam drift, inserting lenses as necessary to limit the maximum beam envelope. However, with space charge, the maximum beam divergence has a strong dependence on the beam radius, using Equation 3.16, as the beam drifts in the Z direction. (We again use conditions appropriate for beams extracted from the RTECR.) To determine the beam radius dependence on drift distance, we integrate Equation 3.16 once with respect to r, and find that

$$\int_{r_m}^{r}\left[\frac{P_\phi^2}{M^2}\left(\frac{1}{r_m^2} - \frac{1}{r^2}\right) + \frac{Q}{\pi M\epsilon_o}\ln\left(\frac{I_i}{v_{zi}}\right)\right]^{-1/2} dr = t \tag{3.17}$$

There exists no analytical solution for the left side of Equation 3.17, but numerical integration techniques can be used to estimate the integral. Let $r = r_m + x$ and assume that x is small (i.e., a short drift distance). Then we have

$$\frac{P_\phi}{M^2}\left(\frac{1}{r_m^2} - \frac{1}{r}\right) + \frac{Q}{\pi M\epsilon_o}\ln(\frac{r}{r_m})\sum(\frac{I_i}{v_{zi}}) \approx x\left[\frac{2P_\phi^2}{M^2 r_m^3} + \frac{Q}{\pi M\epsilon_o r_m}\sum(\frac{I_i}{v_{zi}})\right] \tag{3.18}$$

And by substitution into Equation 3.17 obtains

$$t = \left[\frac{2P_\phi^2}{M^2 r_m^3} + \frac{Q}{\pi M\epsilon_o r_m}\sum(\frac{I_i}{v_{zi}})\right]\int_o^x dx'/x'^{1/2} \tag{3.19}$$

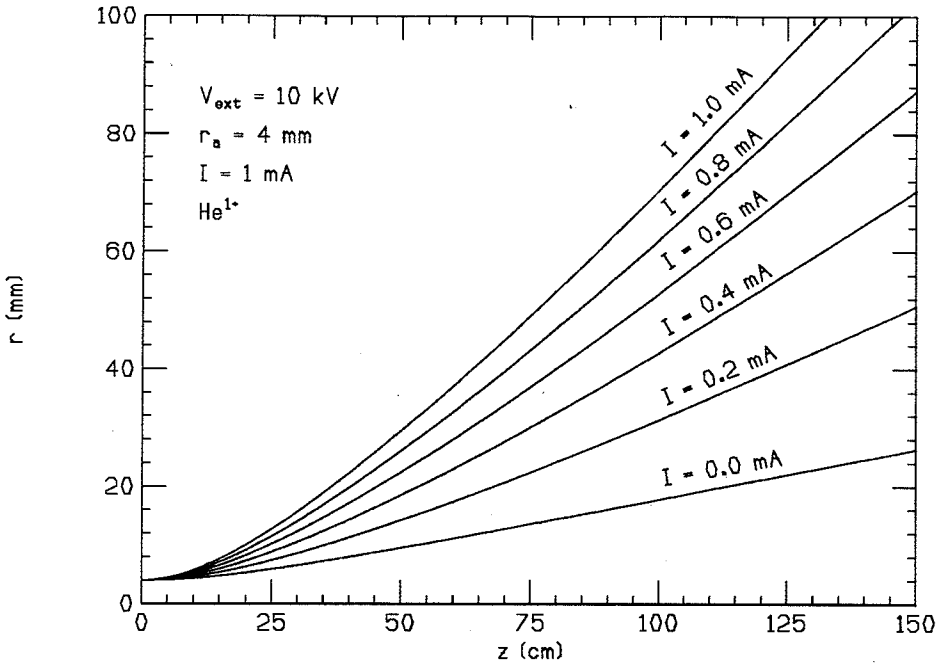

Figure 3.6: The space charge dependence of an ECRIS beam envelope is shown for a 10 kV drifting beam of He^{1+} ion as the intensity is increased.

Performing the integration and rearranging terms yields

$$r - r_m = \frac{1}{4}\left[\frac{2P_\phi^2}{M^2 r_m^3} + \frac{Q}{\pi M \epsilon_o r_m}\sum(\frac{I_i}{v_{zi}})\right]\frac{z^2}{v_z^2} \tag{3.20}$$

Thus in the adiabatic limit, the beam envelope shows a quadratic dependence on the linear drift distance z.

Figure 3.6 shows the growth of a He^+ ion beam envelope for various intensities. In a 1 meter drift, there is a 4-fold increase in beam radius for a 1 emA He^+ beam over a beam with zero net space charge. The consequence of this non-linear radial space charge is that the beam expands faster than would be the case assuming a constant maximum divergence. We conclude that with space charge, both the beam divergence and radius increase with drift distance, as shown schematically in Fig. 3.7. If this is true, then it is likely that the beam envelopes will fill the lenses and bending magnets of the LEBT system, and large emittance growth due to aberrations during each lens transit will occur.

In order to study this phenomena in detail, we developed a new beam code BEAM3D [2]. BEAM3D is a 'single pass' ray tracing code with radial space charge. The space charge is carried by an unlimited number of beamlets. Since ECR sources often have many different charge states extracted simultaneously, BEAM3D allows a charge state distribution to have unlimited charge states. The beam motion integration is written in Cartesian coordinates

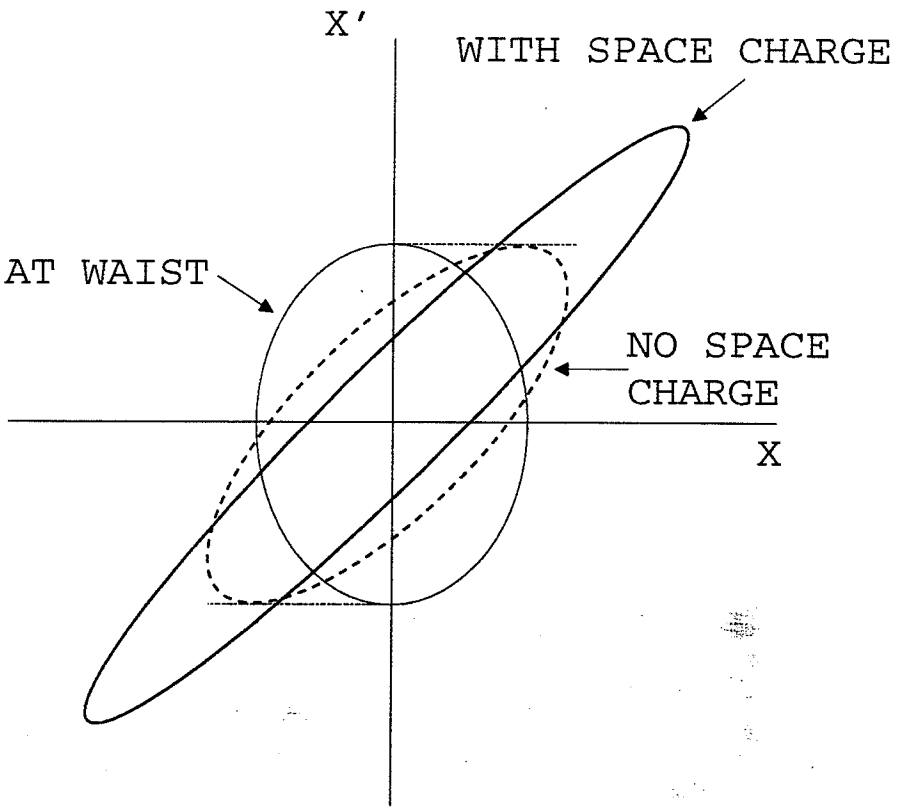

Figure 3.7: If the net space charge is zero, then in a drift after a waist, the growth of the beam envelope is determined by the maximum beam divergence. With space charge, both the beam envelope and divergence are seen to increase with drift distance.

in 3 dimensions, to allow the specification of electric and magnetic fields without requiring symmetries, as well as 3D specification of the beamlet starting conditions. Geometrical structures: slits, caps, etc. that might cut the beam are included, as well as the first element of the LEBT. One can extract $\epsilon_{xx'}, \epsilon_{yy'}, j, n...$ at unlimited arbitrary points along the beam path, in order to compare with measurements. For 5000 rays, BEAM3D requires 4 hours of cpu time on a Vax 8650.

To study the radial space charge question, we simulated with BEAM3D the beam formation process in the RTECR, through the transit of the focussing solenoid, up to the position of the divergence slit box just before the analysis dipole. To study the extraction from the RTECR, we use He^+ beams. We have found that it is possible to tune this ion source to produce He^+ beams over a wide range of intensities, without producing significant He^{2+} intensities, which would complicate the analysis. Helium is the only species for which it is possible to produce an approximately mono-charged total extracted current in the RTECR. With a singly charged extracted current, the total beam characteristics can be studied before the analysis dipole.

Figure 3.8 shows the BEAM3D estimate of emittance envelope growth due to space charge for He^+ beams when crossing the focussing solenoid. This emittance growth is the result of spherical aberration in the solenoid, but due to the space charge growth of the beam envelope before entering the solenoid. As is seen, no emittance growth is observed at $65e\mu A$ intensity, while at 1emA, the emittance growth is nearly 6-fold. Hence theoretically, the radial space charge force could cause a large emittance growth due to aberrations in the transit of the focussing solenoid, but does that happen?

Figure 3.9 shows actual kapton foil burns for $65e\mu A$ and $550e\mu A$ He^+ beams after transit of the solenoid. To make these burns, the beam is passed through a $10cm \times 10cm$ grid of 0.25mm slits and is projected on kapton after a drift of 10cm. Beamlets striking kapton cause a sharp-edged discoloration. The $65e\mu A$ He^+ shows a round image of the RTECR extraction aperture, while the $550e\mu A$ beam completely fills the $10cm \times 10cm$ kapton foil, in good agreement with the prediction of Figure 3.8 . Further, the emittance of the $65e\mu A$ He^+ beam of Figure 3.9 can be extracted from the kapton film. This measured emittance is $69mm \cdot mrad$, accidentally in exact agreement with the starting emittance of Figure 3.8. Such an emittance of $69mm \cdot mrad$ for He^+ extracted from the RTECR would result if the ion beam is cold, corresponding to the cold ion limit given in Equation 3.12. The emittance of the $550e\mu A$ beam cannot be obtained from Fig. 3.9, since the left boundary of the beam cannot be determined, but is greater than $250mm \cdot mrad$.

An intense space charge limited beam would also have, at the dipole entrance, divergence greater than the divergence acceptance. Then the dipole transit would result in further distortion of the beam, and this should also be observable. Figure 3.10 shows the predicted shape and transverse current profiles on an un-neutralized 1 emA He^+ beam traversing a double focussing analysis dipole of the type used at NSCL. Figure 3.10 also shows the collimator surface before the image slit system of such a dipole. As can be seen, the overall image beam shape is triangular, as predicted, with a central beam and a high divergence

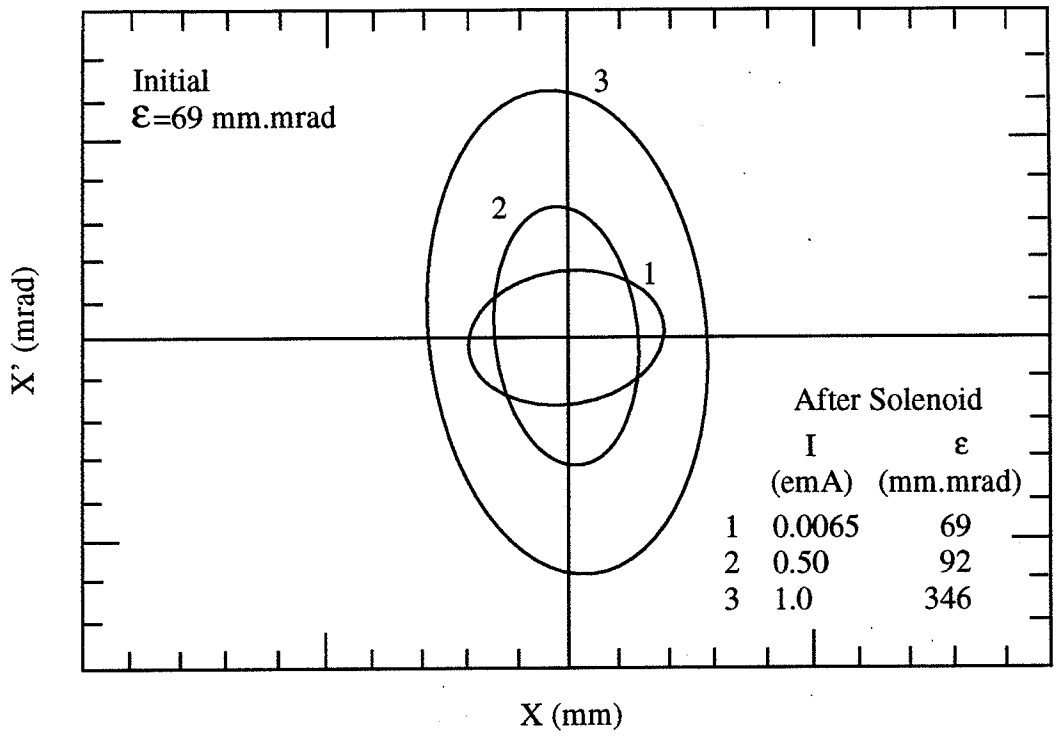

Figure 3.8: The BEAM3D calculated effect of the transit of the first focussing solenoid after the RTECR extraction aperature, for He^+ beams of varying intensity. A clear space charge dependent emittance growth is observed.

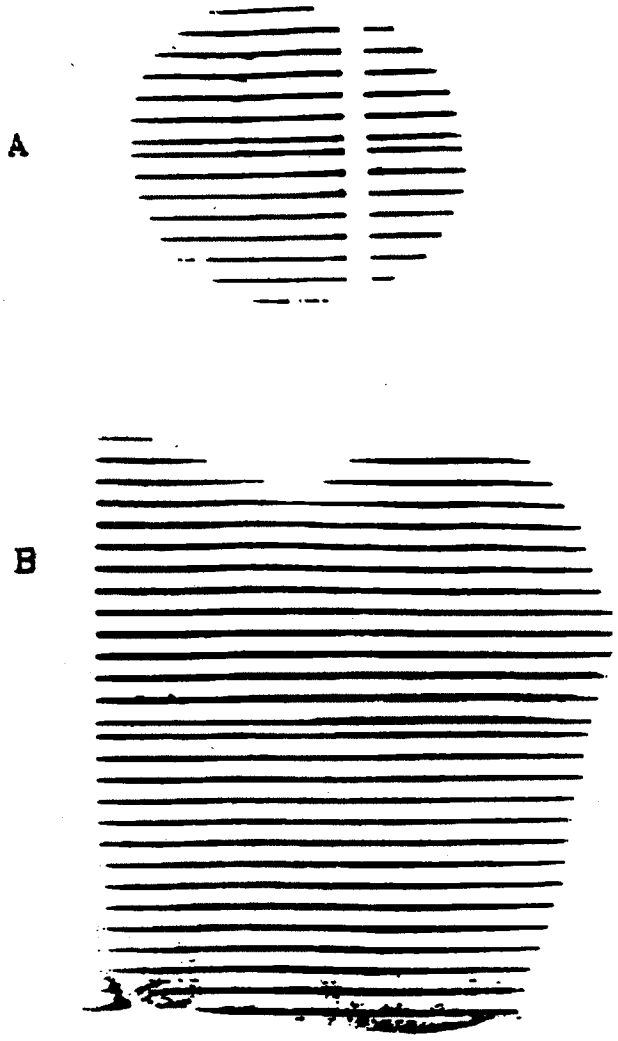

Figure 3.9: The measured relative beam profiles after the transit of the first focussing solenoid after the RTECR extraction, for a) a 65 eμA He^+ beam, and b) a 550 eμA He^+ beam. The prediction of Fig. 3.19 would seem to be confirmed.

tail. We have then strong evidence for space charge effects in the dipole transit as well as the focussing solenoid transit of an ECRIS. Since the total beam intensity is highest here, the largest effects would also be expected in this initial LEBT section.

To summarize, we have strong evidence for space charge limited beam transmission in the RTECR analysis system. To improve the transmission, we should reduce the drift distances, since according to Equation 3.20, the beam envelope will have a quadratic dependence on drift distance. The drift to the first solenoid is the most important, since the total extracted current from the source is present. As a first application of these concepts, we redesigned the first solenoid transit of the SCECR, then under construction. (At that time, the RTECR was too heavily used to permit a disruption to change the initial drift.) Figure 3.11 shows a comparison of the initial focussing magnets of the RTECR and the SCECR. By increasing the strength of the SCECR focus, we could reduce the overall drift distance by about 50%. BEAM3D calculations were performed on this new configuration and predicted no spherical aberration effects in intense beam transit of this magnet. With divergence growth minimized, a 'clean' transit of the analysis dipole was also expected. Figure 3.12 shows a comparison of Argon emittance measurements of these two ion sources at a bias voltage of 10 kV. The 100% emittance contour of the SCECR is significantly lower than that of the RTECR, as expected on the basis of controlling space charge effects. The large emittance growth of the RTECR for 100% intensity (over 90%), is the consequence of the triangular distortion of the beam in the transit of the dipole.

3.3.3. Proper LEBT for High Space Charge Beams

The main point here is that dc beams extracted from ECRIS, like the RTECR, do not neutralize. Then the beam envelope growth will depend quadratically on the drift distance z in the LEBT: $\Delta r \propto \Delta z^2$. Nearly all LEBT designs for presently operating ECRIS have the implicit assumption that $\Delta r \propto \alpha \Delta z$, where α is the starting transverse divergence. Hence, in these systems, all focussing magnets are too far 'downstream'. The beam envelopes are then larger than anticipated, filling magnet apertures, resulting in aberrations and a dilution of the phase space, lowering the overall LEBT transmission. The successful initial beam transport system for the SCECR, designed for high intensity, is a direct confirmation of the importance of including space charge in the LEBT design.

To summarize our current understanding of ECR extraction and LEBT (including other aspects not discussed here):

1. Beam extraction follows Pierce Theory up to a tune saturated current limit ($I \propto V^{3/2}$).

2. Assuming a flat plasma emission surface in the simulations best fits experimental measurements of the initial beam properties.

3. $T_Q \leq 10eV \times Q$.

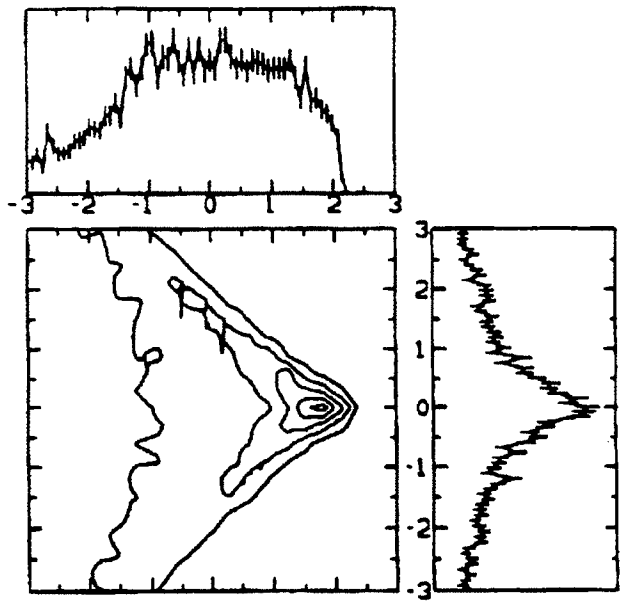

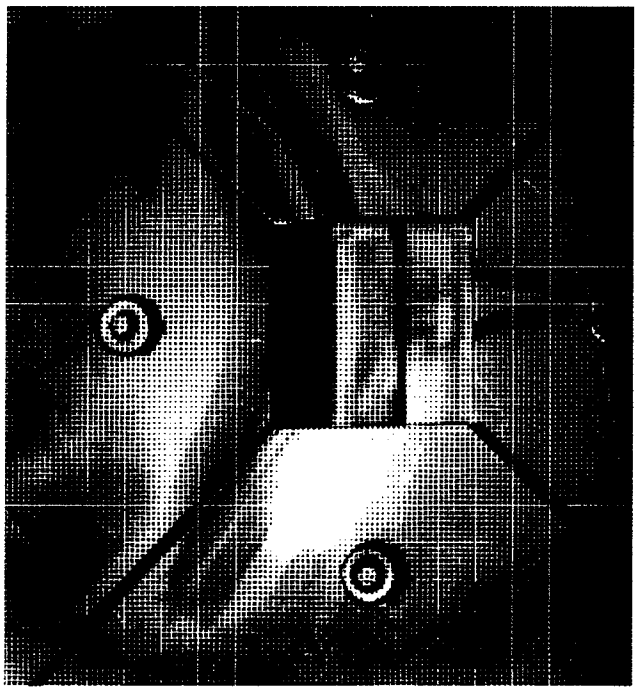

Figure 3.10: An azimuthally symmetric He^+ beam from an ECRIS is made triangular by second order aberrations in the transit of a dipole magnet, as both space charge calculations and measured dipole image of a 1 emA beam show.

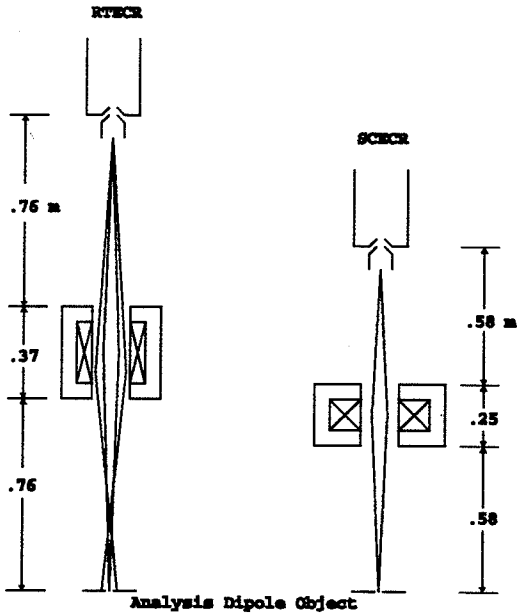

Figure 3.11: A comparison of the initial drift and focussing lens after the RTECR and SCECR ion sources.

4. ϵ_x and ϵ_y are dominated by A_ϕ.

5. Extracted beams appear to have low neutralization, and LEBT designs must include compensation for the assumed final space charge operating level.

3.4. Beam Diagnostic Requirements and Auxiliary Hardware

While the present K500 injection line was built and operated first, the K1200 injection line has seen more beam diagnostic and control development. We would apply these developments to the new K500 high intensity injection line. These developments include:

1. For beam centering and transmission optimization: fast position sensitive sectored faraday cups with a graphical beam density display

2. To monitor and correct emittance growth: emittance measurements for the initial analyzed beams, near the end of the horizontal line, and on the cyclotron axis

3. For beam injection optimization: a direct inflector (anode) current monitor mode

4. For precise beam intensity control: fixed beam intensity attenuators- 1/3, 1/10, 1/33 ... 10^{-9}

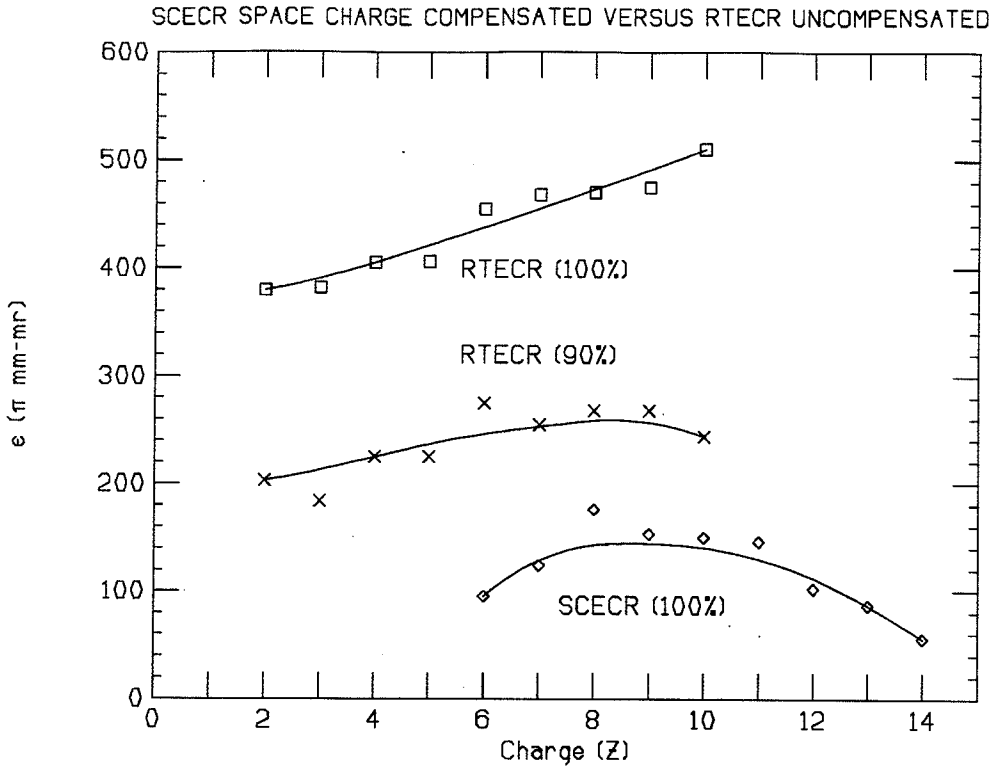

Figure 3.12: As a consequence of better initial space charge compensation, the measured SCECR emittances are significantly lower than the RTECR.

5. Radiation safety beam stop

6. User lockout beam stop

Several diagnostic boxes will be needed in the injection line design in order to install this hardware. The new injection line will require several transverse steering elements to maintain the beam centering. An existing steering magnet design, used in the present injection lines, will be sufficient for this purpose [31]. The present beam lines have a 6 inch bore coupled with metal seals. This permits high vacuum ($\approx 10^{-8}$ Torr) to be maintained with a small number of turbomolecular pumps ($\sim$1 pump / 10 m). Subject to constraints imposed by the focussing element design, we will try to follow this design.

4. Proposed K500 High Intensity Injection Line

Figure 4.1 shows the proposed K500 high intensity injection line, as well as the ion source configuration and the initial K1200 beam transport line. The SCECR remains in its present location as does the existing SCECR/K1200 injection line. The RTECR has been upgraded to the High B mode and moved closer to the K500, with an angular offset from the main line equal to that of the SCECR. For space charge compensation, the length of the injection line is minimized, and the level of focussing increased to approximately twice that in the existing

line. To minimize the length, the line has been straightened. This will require cutting a new entrance to the cyclotron vault, and altering the design of the final bending magnet to minimize interference with the C lower resonator. The beam analysis systems of the SCECR and upgraded RTECR are identical but separate – to permit independent tuning and optimization. After analysis, beams of fixed M/Q from either source are merged into the main horizontal transport structure. This consists of a sequence of focussing solenoids, steering magnets and diagnostic boxes. These boxes will contain the faraday cups, beam stops and beam attenuator grids. The attenuator grids are distributed over several boxes with the focussing elements in between to eliminate systematic alignment effects. After the horizontal transport section, the beam is bent to the cyclotron axis. The beam box above the last dipole magnet is the location of the matching point for axial injection.

Azimuthally symmetric focussing elements are preferred over quadrupoles in this LEBT for several reasons. First, ECRIS initial beams have azimuthal symmetry. Focussing solenoids are then sufficient if this symmetry is preserved and this makes the injection line tuning operationally simple. In addition, for this line, space charge is important, and with space charge the sequential focussing nature of quadrupole doublets generally introduces an asymmetry that may result in significant phase space distortions. Finally, for quadrupole focussing, more elements are required and generally less aperture is available for a given focussing strength. More elements increases building and operating costs, but so does less aperture – conductance is reduced and that increases vacuum hardware requirements.

LEBT systems can of course be built with electrostatic elements. In principle, electrostatic elements are cheaper and easier to build. Einsellenses would be the azimuthally symmetric electric analog of the focussing solenoids. Einsellenses are weak, second order focussing systems and require an operating voltage of the order of the beam voltage. For a 30 kV injection line this may be a problem. At Atlas, the ECRIS operating voltage is limited to about 12 kV due to Einsellense voltage limitations [32]. Additionally, the electric analog of magnetic rigidity is independent of mass – all ions of the same charge will be focussed. An important feature of the first focussing element after the ECRIS extraction is to partially eliminate unwanted ions to reduce space charge, so this feature of electrostatic lenses is undesirable. Finally, electrostatic elements suppress beam neutralization, should any be present.

Figure 4.2 shows a second order transport calculation for 30 kV/Q O^{3+} ions transported from the SCECR to the K500. (The merging magnet is not present in this calculation - we focus through it in any case.) For this calculation, the starting transverse emittance is symmetric and $5 \cdot 20\pi mm.mrad$. The first two magnets (a solenoid and a 90° dipole) comprise the ECRIS/LEBT matching and ECRIS charge selection systems. The desired ion is coarsely selected after the solenoid, reducing the total space charge by a much as 70%. This solenoid is the same as that shown previously in Figure 3.11, and generally credited with significantly improving the space charge matching of the SCECR to the existing LEBT system. The final charge selection is obtained in slits placed at the first dipole image. For an intense multiply-charged ion source like the SCECR, the optimum space charge matching is

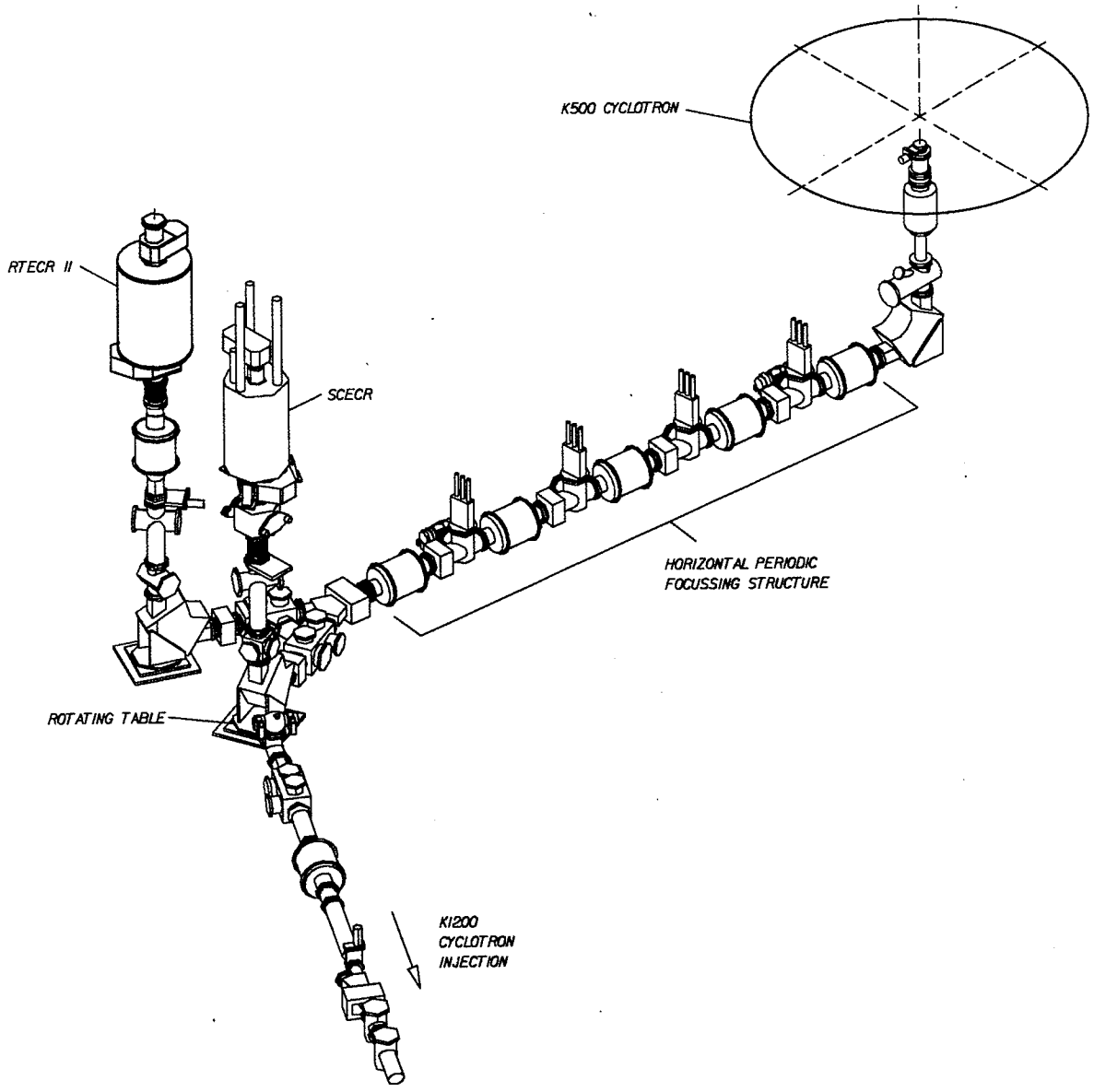

Figure 4.1: The proposed K500 LEBT system with the SCECR and enhanced High B RTECR. Provision is retained for direct beam injection of the K1200 cyclotron from the SCECR, through a rotation of the SCECR analysis magnet.

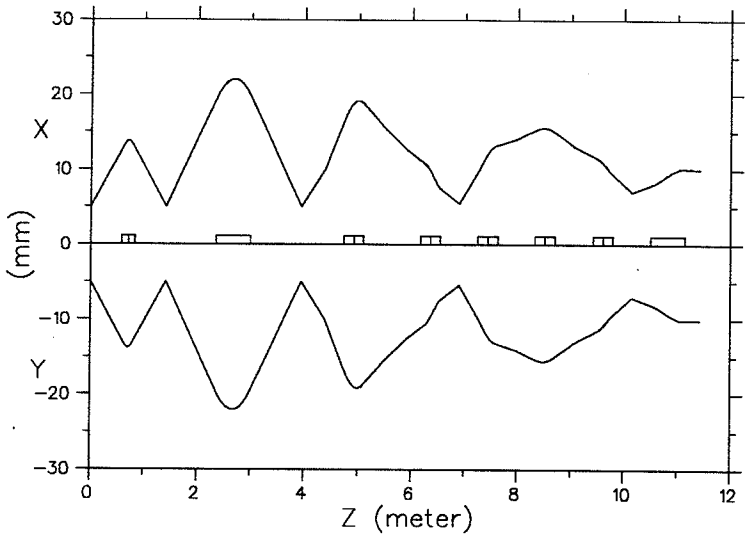

Figure 4.2: A zero space charge second order Transport calculation for the proposed new injection line for the K500 cyclotron.

difficult to achieve over the whole operating range of the ion source. The main consequence of bad matching is excessive initial beam divergence. To improve on the matching, the pole gap and width of the analysis dipole will be increased to improve the good field region while preserving other characteristics. The 6 inch bore solenoids in the horizontal line after the first dipole are the same as those used in the present injection lines [33]. The number used for focussing is increased to the maximum possible, while still allowing space for steering magnets and beam diagnostics. This distributed, periodic focussing structure allows both a larger minimum beam radius (to reduce the space charge force), and a smaller maximum beam radius (to suppress third order aberrations), than in the present injection line. At present, the final dipole is a double focussing magnet like the analysis dipole, but we are looking at alternatives – the edge angles are not as effective in the cyclotron fringe field, and there is not sufficient space to increase the pole gap to reduce second order aberrations.

This high intensity LEBT design for the K500 is primarily an extension of the analysis that led to a suppression of space charge effects in the SCECR analyzed beams, and we expect a significant improvement in transport efficiency over the existing LEBT design as a consequence. Using this transport calculation as a starting point, we have made a preliminary check of high space charge transport with Parmila, presented in Figure 4.3. According to Parmila, it should be possible to transport a 1 emA O^{3+} beam from the SCECR to the cyclotron match point without space charge induced aberrations. This result is encouraging. We believe that we have a reasonable understanding of the beam formation and mass analysis

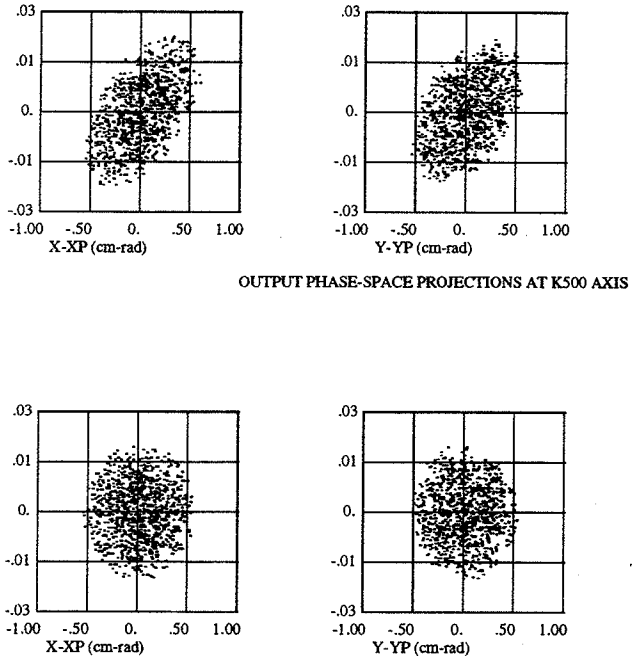

Figure 4.3: Parmila shows little transverse emittance growth for a 1.0 emA oxygen 3+ beam transported from the SCECR to the axis of the K500 cyclotron.

of the SCECR. After analysis, beam transport occurs with a single q/m, and for the net space charge Parmila should be applicable – while Parmila has not been used extensively for multiply-charged LEBT applications, it has widespread used for intense H^+/H^- LEBT transport to LINACS [34].

5. Acknowledgments

The author would like to acknowledge significant help in the preparation of this report. First, thanks to the NSCL Ion Source group, particularly Dallas Cole and Keith Harrison, for keeping the ECR/K1200 effort going forward during this time. Many of the figures, particularly the new beam measurements, have been 'pre-extracted' from Keith Harrison's thesis – that effort is going well, and he will soon be a fine addition to Richard Geller's *Club R.C.E.* Sarah Alfredson was essential to the successful assembly of this report – her mastery of software and hardware for data analysis and document preparation is the reason that anything we do with the ion sources here makes it to print. Finally, thanks to L. Harwood, A. Zeller and J. Nolen – the architects of the original injection lines for ECRIS at NSCL, the basis for the present work.

6. References

References

[1] T.A. Antaya and S. Gammino. The scecr high b mode and frequency scaling in ecr ion sources. In *5th International Conference on Ion Sources*, Beijing, P.R.C, 1993. to be published.

[2] Z.Q. Xie and T.A. Antaya. The effect of space charge on beams extracted from the room temperature electron cyclotron resonance ion source (abstract). In *International Conference on Ion Sources*, page 341, Berkeley, California, 1989.

[3] T.A.Antaya, D. Cole, P. Miller, and D. Poe. K1200 beam development techniques. In *Proceedings of the 13th International Conference on Cyclotrons and Their Applications*, pages 427–430, World Scientific Co, Singapore, 1992.

[4] Z.Q. Xie. *The Effect of Space Charge Force on Beams Extracted from ECR Ion Sources.* PhD thesis, MIchigan State University, East Lansing, MI 48824, September 1989.

[5] T.A.Antaya and D. Cole. The super gas mixing technique for highly charged uranium ions. In *Proceedings of the 13th International Conference on Cyclotrons and Their Applications*, pages 348–351, World Scientific Co, Singapore, 1992.

[6] J. Arge, V. Nieminen, P. Heikkinen, E. Liukkonen, A. Backlin, and S. Holm. Status of the jyvaskyla-uppsala ecr ion source project. In *International Conference on ECR Ion Sources and Their Applications*, pages 296–299, East Lansing, Michigan, 1987.

[7] S. Holm. Operational experience of the reconstructed uppsala synchrocyclotron. In *12th International Conference on Cyclotrons and Their Applications*, pages 17–20, Berlin, Germany, 1989.

[8] D.K. Bose and T.A. Antaya. The design of a compact two stage (compact plus) e.c.r. ion source. In *International Conference on ECR Ion Sources and Their Applications*, pages 371–379, East Lansing, Michigan, 1987.

[9] G. Ciavola and S. Gammino. A superconducting electron cyclotron resonance source for the l.n.s. In *Proceedings of the 4th International Conference on Ion Sources*, pages 2881–2882, Bensheim, Germany, 1991.

[10] R. Geller. Electron cyclotron resonance (e.c.r.) multiple charged ion sources. In *Eighth International Conference on Cyclotrons and Their Applications*, pages 2120–2127, Bloomington, Indiana, 1978.

[11] Y. Jongen and G. Ryckewaert. Initial operation of e.c.r. ion sources with cyclone. In *1983 Particle Accelerator Conference Accelerator Engineering and Technology*, pages 2685–2689, Santa Fe, New Mexico, 1983.

[12] T.A. Antaya. The atomic nature of the ion production limit in ecr ion sources. In *VIth International Conference on the Physics of Highly Charged Ions*, pages 653–662, Manhattan, Kansas, 1992.

[13] C. Barue, P. Briand, A. Girard, G. Melin, and G. Brifford. Hot electron studies in the minimafios ecr ion source. In *Proceedings of the 4th International Conference on Ion Sources*, pages 2844–2846, Bensheim, Germany, 1991.

[14] G. Melin, D. Hitz, M. Pontonnier, and T.K. Nguyen. New results and evolution of the caprice ecr ion source concept. In *Proceedings of the 11th Iternational Workshop on Electron Cyclotron Resonance Ion Sources (ECRIS 11)*, pages 91–96, Groningen, The Netherlands, 1993.

[15] T. Nakagawa, T. Kageyamam, A. Goto, M. Kase, Y. Kanai, Y. Nakai, and Y. Yano. Plasma cathode method for riken 10 ghz ecris. In *Proceedings of the 11th Iternational Workshop on Electron Cyclotron Resonance Ion Sources (ECRIS 11)*, pages 208–212, Groningen, The Netherlands, 1993.

[16] C.M. Lyneis, Z.Q. Xie, D.J. Clark, R.S. Lam, and S.A. Lundgren. Preliminary performance of the lbl aecr. In *Proceedings of the 10th International Conference on ECR Ion Sources*, pages 47–62, Oak Ridge, Tennessee, 1991.

[17] H. Beuscher. Status of the 14 ghz julich ecris. In *Proceedings of the International Conference on the Physics of Mulitply Charged Ions ant International Workshop on ECR Ion Sources*, pages 883–886, Grenoble, France, 1988.

[18] Y. Jongen. Electron cyclotron resonance (e.c.r.) ion sources. In *10th International Conference on Cyclotrons and Their Applications*, pages 322–327, East Lansing, Michigan, 1984.

[19] R. Geller, F. Bourg, J. Debernardi, B. Jacquot, R. Pauthenet, M. Pontonnier, and P. Sortais. The minimafios status 1985. In *Workshop on the Sixth International ECR Ion Source*, pages 1–27, Berkeley, California, 1985.

[20] T.A. Antaya. A review of studies for the variable frequency superconducting ecr ion source project at msu. In *Proceedings of the International Conference on the Physics of Multiply Charged Ions and International Workshop on ECR Ion Sources*, pages 707–726, Grenoble, France, 1988.

[21] T.A. Antaya, S. Gammino, C. Ciavola, and M. Loiselet. Selective enhancement of highly charged ions extracted from the scecr ion source. In *Proceedings of the Third International Conference on Radioactive Nuclear Beams*, pages 127–134, Edition Frontieres, France, 1993.

[22] R. Pardo, 1993. private communication.

[23] S.T. Yennello and et. al. New nuclei near the proton dripline around z=40. *Physical Review C*, 46:2620, 92.

[24] D.J. Clark, Y. Jongen, and C.M. Lyneis. Progress on the lbl ecr heavy ion source. In *Tenth International Conference on Cyclotrons and Their Applications*, pages 133–136, East Lansing, Michigan, 1984.

[25] T.A. Antaya. Initial results with a vertical, full iron yoke, 2 x 6.4 ghz ecr source for the nscl heavy ion cyclotrons. In *Contributed Papers of the 7th Workshop on ECR Ion Sources*, pages 72–102, Julich, Germany, 1986.

[26] C.M. Lyneis and T.A. Antaya. Ecr sources for the production of highly charged ions. In *International Conference on Ion Sources*, pages 221–224, Berkeley California, 1989.

[27] MSU/NSCL. Beamlist, March 1992.

[28] R. Geller. private communication.

[29] E. Baron. High intensity and space charge problems at ganil. In *Eleventh International Conference on Cyclotrons and Their Applications*, pages 234–237, Tokyo, Japan, 1986.

[30] L.H. Harwood, J.A. Nolen, S. Tanaka, and A.F. Zeller. Analysis and transport of beams from the ecr ion source to the nscl k500 and k800 cyclotrons. In *Eleventh International Conference on Cyclotrons and Their Applications*, pages 488–494, Tokyo, Japan, 1986.

[31] M.F. Williams, A.F. Zeller, and J.A. Nolen. Ecr beamline x-y steering magnets. In *MSU/NSCL Annual Report*, pages 172–175, East Lansing, Michigan, 1985.

[32] J. Nolen, 1994. private communication.

[33] A.F. Zeller, J.A. Nolen, and R.T. Swanson. Ecr beamline solenoids. In *MSU/NSCL Annual Report*, pages 170–171, East Lansing, Michigan, 1985.

[34] G. Boicourt and J. Merson. Parmila users and reference manual. Technical Report LA-UR-90-127, Los Alamos National Laboratory (LANL), University of California, September 1990.